

Storage, Computation, and Communication: A Fundamental Tradeoff in Distributed Computing

Qifa Yan, Sheng Yang, and Michèle Wigger

Abstract

Distributed computing has become one of the most important frameworks in dealing with large computation tasks. In this paper, we investigate a MapReduce like distributed computing system. Our main contribution is the characterization of the optimal tradeoff between storage space, computation load, and communication load. To this end, we derive an information-theoretical converse and show that time- and memory- sharing between the operating points achieved by the modified coded distributed computing (M-CDC) scheme proposed by Ezzeldin *et al.* attains all the points on this tradeoff. Our result thus extends the result by Li *et al.* on the optimum tradeoff between storage and communication to account also for the computation load. We further show how to obtain a distributed computing scheme from any *placement delivery array (PDA)* whose ordinary symbols occur at least twice. Previously proposed PDAs to solve the subpacketization problem in coded caching by Yan *et al.* and Shangguan *et al.* allow us then to derive optimal distributed computing schemes that require only a small number of files, and thus have reduced complexity.

Index Terms

Distributed computing, storage, communication, MapReduce, placement delivery array

I. INTRODUCTION

Massively large distributed systems have emerged as one of the most important forms to run big data and machine learning algorithms, so that data-parallel computations can be executed accross clusters of many individual computing nodes. In particular, distributed platforms like MapReduce [1], Dryad [2] *et al.* have become popular and can handle computing tasks involving data sizes as large as tens of terabytes. As illustrated in Fig. 1, computations in these systems are typically decomposed into “map” functions and “reduce” functions as detailed in the following.

Consider the task of computing K output functions at K nodes and that each output function is of the form

$$\phi_k(w_1, \dots, w_N) = h_k(g_{k,1}(w_1), \dots, g_{k,N}(w_N)), \quad k = 1, \dots, K. \quad (1)$$

Q. Yan and M. Wigger are with LTCI, Télécom ParisTech, Université Paris-Saclay, 75013 Paris, France. E-mails: qifa.yan@telecom-paristech.fr, michele.wigger@telecom-paristech.fr.

S. Yang is with L2S, (UMR CNRS 8506), CentraleSupélec-CNRS-Université Paris-Sud, 91192 Gif-sur-Yvette, France. Email: sheng.yang@centralesupelec.fr.

Part of this paper will be presented in 2018 IEEE Information Theory Workshop (ITW).

Here, each output function ϕ_k depends on all N data blocks w_1, \dots, w_N , but can be decomposed into:

- N *map functions* $g_{k,1}, \dots, g_{k,N}$, each only depending on one block;
- a *reduce function* h_k that combines the outcomes of the N map functions.

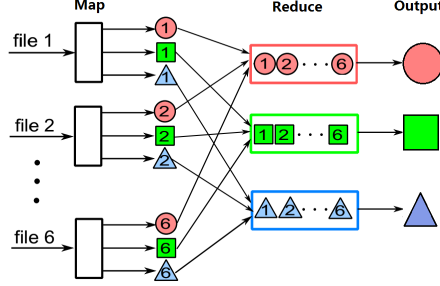


Fig. 1: A computing task with $N = 6$ files and $K = 3$ output functions. The small and big red circles, green squares and blue triangles denote IVAs and results belonging to different output functions.

Computation of such functions can be performed in a distributed way following 3 phases: In the first *map phase*, each node $k = 1, \dots, K$ locally stores a subset of the input data $\mathcal{M}_k \subseteq \{w_1, \dots, w_N\}$, and calculates all *intermediate values* (IVAs) that depend on the stored data:

$$\mathcal{C}_k \triangleq \{g_{q,n}(w_n) : q \in \{1, \dots, K\}, n \in \mathcal{M}_k\}. \quad (2)$$

In the subsequent *shuffle phase*, the nodes exchange the IVAs computed during the map phase, so that each node k is aware of all the IVAs $g_{k,1}(w_1), \dots, g_{k,N}(w_N)$ required to calculate its own output function ϕ_k . In the final *reduce phase*, each node k combines the IVAs with the reduce function h_k as indicated in (1).

Recently, Li *et al.* [3] proposed a scheme, termed *coded distributed computing (CDC)*, that in the map phase stores files multiple times across users so as to enable multicast opportunities for the shuffle phase. This approach can significantly reduce the communication load over traditional uncoded schemes as illustrated in Fig. 2, and was proved in [3] to have the smallest communication load among all the distributed computing schemes with same total storage requirements. It is worth mentioning that Li *et al.* in [3] used the term *computation-communication* tradeoff, because they assumed that each node calculates all the IVAs that can be obtained from the data stored at that node, irrespective of whether these IVAs are used in the sequel or not. In this sense, the total number of calculated IVAs is actually a measure of the total storage space consumed across the nodes. This is why we would rather refer to it as the *storage-communication* tradeoff. In this context, it is natural to investigate a more general framework, where each node is allowed to choose for each IVA that it can calculate from its locally stored data, whether or not to perform this calculation. The number of IVAs effectively calculated at all the nodes, normalized by the total number of IVAs, is then used to measure the real computation load. In this sense, we extend the storage-communication tradeoff in [3] to a *storage-computation-communication* tradeoff. That means, our goal is to identify all storage-computation-communication (SCC) triples, for which the task of computing the K output functions in (1) can be accomplished.

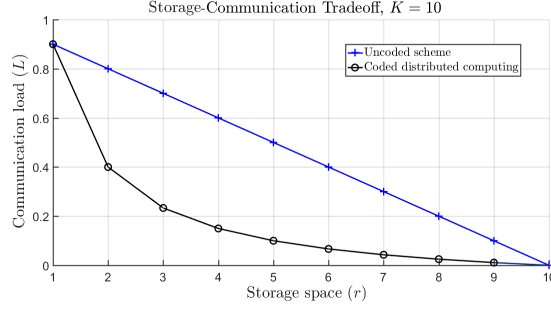


Fig. 2: Comparison of CDC scheme and uncoded scheme for a task of computing $K = 10$ output functions.

In this work, we fully characterize all feasible SCC triples, and as a consequence, the pareto-optimal tradeoff surface. We show that any feasible triple on this optimal tradeoff surface can be attained by time- and memory-sharing different operating points of the modified CDC (M-CDC) scheme proposed in [4]. The M-CDC modifies the CDC scheme in that each node only computes the IVAs that it will be using in subsequent phases. Our information-theoretical converse proves optimality of the described SCC-triples.

We thus extend the Li *et al.* work in [3] to not only account for storage space and communication load, but also for computation load. Other extensions have recently been proposed. For example, [5]–[14] included straggler nodes but restricted to map functions that are matrix-vector or matrix-matrix multiplications; straggler nodes with general linear map functions were considered in [15]; [16] studied optimal allocation of computation resources; [17]–[20] investigated distributed computing in wireless networks; [21]–[23] investigated the iterative procedures of data computing and shuffling; [24] studied the case when each node has been randomly allocated files; [25] investigated the case with random connectivity between nodes; [26]–[29] designed codes for computing gradient distributedly, which is particularly useful in machine learning.

One major practical limitation of distributed computing schemes like CDC or M-CDC is that they can only be implemented if the number of files N is large, with respect to the number of computing nodes K . This problem is somehow reminiscent of the high subpacketization level of most proposed coded caching schemes [30]. Interestingly, the tool derived by Yan *et al.* to solve the subpacketization problem for coded caching also allows to reduce the number of files required for distributed computing. This tool is the placement delivery array (PDA), which was introduced in [31] to represent both placement and delivery of coded caching schemes with uncoded prefetching in a single array. In PDAs used for coded caching, each column is identified with a different cache-aided user and each row with a different subpacket of the files. In this paper, we show that PDAs whose ordinary symbols occur at least twice can also be used to represent the map, shuffle, and reduce procedures of distributed computing. Moreover, *almost-regular PDAs*, i.e., PDAs whose ordinary symbols all occur g or $g+1$ times, for some $g \in \{2, 3, \dots, K-1\}$, correspond to distributed computing schemes with optimal storage-computation-communication load. Notice that for distributed computing, each column of a PDA is identified with a different node in the system and each row is identified with a different batch of files. Since each batch contains at least one file, the number of rows of the PDA indicates the minimum number of files required to implement the corresponding distributed computing scheme.

Thus, in order to solve the number-of-files problem, it suffices to present almost-regular PDAs with few rows. Such PDA constructions have been proposed in [31] and [32] with the goal to solve the subpacketization problem for coded caching. In this paper, we explicitly derive the performance of the PDA constructions presented in [31] and [32] and prove the following findings. When using the PDA constructions in [31], the required number of files is in the order of $O\left(e^{K \cdot \frac{1}{q} \ln q}\right)$ files, where q is an integer that factorizes K . With the PDA constructions in [32], even a sub-exponential number of files in K suffices, when storage space is large. To compare, the CDC and M-CDC schemes require in the order of $O\left(e^{K\left(\frac{1}{q} \ln q + \left(1 - \frac{1}{q}\right) \ln \frac{q}{q-1}\right)}\right)$ files, where again q is an integer that factorizes K .

The remainder of this paper is organized as follows. The problem is formulated in Section II; the *fundamental SCC region and the optimal tradeoff surface are presented in Section III*; the proofs of these results are provided in Section IV and the appendices; Section V characterizes the computing schemes by PDAs, and obtains schemes requiring smaller number of files from this characterization; and Section VI concludes the paper.

Notations: Let \mathbb{N}^+ be the set of positive integers. For $m, n \in \mathbb{N}^+$, denote the n -dimensional vector space over the finite field with cardinality 2^m by $\mathbb{F}_{2^m}^n$, and the integer set $\{1, \dots, n\}$ by $[n]$. We denote $f(n) = \Theta(g(n))$ if there exist positive constants a, b such that $ag(n) \leq f(n) \leq bg(n)$. If $m < n$, we use $[m : n]$ to denote the set $\{m, m+1, \dots, n\}$. We also use interval notations, e.g., $[a, b] \triangleq \{x : a \leq x \leq b\}$ and $[a, b) \triangleq \{x : a \leq x < b\}$ for real numbers a, b such that $a < b$. The bitwise exclusive OR (XOR) operation is denoted by \oplus .

To denote scalar or vector quantities we use the standard font, e.g., a or A , for arrays we use upper case bold font, e.g., \mathbf{A} , for sets we use upper case calligraphic font, e.g., \mathcal{A} , and for collections (sets of sets) we use upper case Greek letters with bold font, e.g., $\mathbf{\Omega}$.

A line segment with end points A_1, A_2 or a line through the points A_1, A_2 is denoted by $\overline{A_1 A_2}$. A triangle with vertices A_1, A_2, A_3 is denoted by $\triangle A_1 A_2 A_3$. A trapezoid with the four edges $\overline{A_1 A_2}$, $\overline{A_2 A_3}$, $\overline{A_3 A_4}$, and $\overline{A_4 A_1}$, where $\overline{A_1 A_2}$ is parallel to $\overline{A_3 A_4}$ is denoted by $\square A_1 A_2 A_3 A_4$. Let \mathcal{F} be a set of facets, if the facets in \mathcal{F} form a continuous surface, then we refer to this surface simply as \mathcal{F} .

II. PROBLEM SETUP

Consider a system consisting of K distributed computing nodes

$$\mathcal{K} \triangleq \{1, \dots, K\} \quad (3)$$

and N files,

$$\mathcal{W} = \{w_1, \dots, w_N\}, \quad w_n \in \mathbb{F}_{2^D}, \forall n \in [N], \quad (4)$$

each of size D bits, where $K, N, D \in \mathbb{N}$. The goal of node k ($k \in \mathcal{K}$) is to compute an output function¹

$$\phi_k : \mathbb{F}_{2^D}^N \rightarrow \mathbb{F}_{2^B}, \quad (5)$$

¹See Remark 1 for a relaxed assumption.

which maps all the files to a bit stream

$$u_k = \phi_k(w_1, \dots, w_N) \in \mathbb{F}_{2^B} \quad (6)$$

of length B , for a given $B \in \mathbb{N}$.

Following the conventions in [3], we assume that each output function ϕ_k decomposes as:

$$\phi_k(w_1, \dots, w_N) = h_k(g_{k,1}(w_1), \dots, g_{k,N}(w_N)), \quad (7)$$

where:

- Each “map” function $g_{k,n}$ is of the form

$$g_{k,n} : \mathbb{F}_{2^D} \rightarrow \mathbb{F}_{2^T}, \quad (8)$$

and maps the file w_n into the IVA

$$v_{k,n} \triangleq g_{k,n}(w_n) \in \mathbb{F}_{2^T}, \quad (9)$$

for a given $T \in \mathbb{N}$.

- The “reduce” function h_k is of the form

$$h_k : \mathbb{F}_{2^T}^N \rightarrow \mathbb{F}_{2^B}, \quad (10)$$

and maps the IVAs

$$\mathcal{V}_k \triangleq \{v_{k,n} : n \in [N]\} \quad (11)$$

into the output stream

$$u_k = h_k(v_{k,1}, \dots, v_{k,N}). \quad (12)$$

Notice that such a decomposition always exists. For example, let the map functions be identity functions and the reduce functions be the output functions, i.e., $g_{k,n}(w_n) = w_n$, and $h_k = \phi_k$, $\forall n \in [N]$, $k \in \mathcal{K}$.

The described structure of the output functions ϕ_1, \dots, ϕ_K , allows the nodes to perform their computation in the following three-phase procedure.

1) **Map Phase:** For each $k \in \mathcal{K}$, node k chooses to store a subset of files $\mathcal{M}_k \subseteq \mathcal{W}$. For each file $w_n \in \mathcal{M}_k$, node k computes a subset of IVAs

$$\mathcal{C}_{k,n} = \{v_{q,n} : q \in \mathcal{Z}_{k,n}\}, \quad (13)$$

where $\mathcal{Z}_{k,n} \subseteq \mathcal{K}$. Denote the set of IVAs computed at node k by \mathcal{C}_k , i.e.,

$$\mathcal{C}_k \triangleq \bigcup_{n:w_n \in \mathcal{M}_k} \mathcal{C}_{k,n}. \quad (14)$$

2) **Shuffle Phase:** The K nodes exchange some of their computed IVAs. In particular, node k creates a signal

$$X_k = \varphi_k(\mathcal{C}_k) \quad (15)$$

of some length $l_k \in \mathbb{N}$, using a function

$$\varphi_k : \mathbb{F}_{2^T}^{|\mathcal{C}_k|} \rightarrow \mathbb{F}_{2^{l_k}}. \quad (16)$$

It then multicasts this signal to all the other nodes, which receive it error-free.

3) **Reduce Phase:** Using the shuffled signals X_1, \dots, X_K and the IVAs \mathcal{C}_k it computed locally in the map phase, node k now computes the IVAs

$$(v_{k,1}, \dots, v_{k,N}) = \psi_k(X_1, \dots, X_K, \mathcal{C}_k), \quad (17)$$

for some function

$$\psi_k : \mathbb{F}_{2^{l_1}} \times \mathbb{F}_{2^{l_2}} \times \dots \times \mathbb{F}_{2^{l_K}} \times \mathbb{F}_{2^T}^{|\mathcal{C}_k|} \rightarrow \mathbb{F}_{2^N}^N. \quad (18)$$

Finally, it computes

$$u_k = h_k(v_{k,1}, \dots, v_{k,N}). \quad (19)$$

To measure storage, computation, and communication costs of the described procedure, we introduce the following definitions.

Definition 1 (Storage Space). Storage space r is defined as the total number of files stored across the K nodes normalized by the total number of files N :

$$r \triangleq \frac{\sum_{k=1}^K |\mathcal{M}_k|}{N}. \quad (20)$$

Definition 2 (Computation Load). Computation load c is defined as the total number of map functions computed across the K nodes, normalized by the total number of map functions NK :

$$c \triangleq \frac{\sum_{k=1}^K |\mathcal{C}_k|}{NK}. \quad (21)$$

Definition 3 (Communication Load). Communication load L is defined as the total number of the bits sent by the K nodes during the shuffle phase normalized by the total length of all intermediate values NKT :

$$L = \frac{\sum_{k=1}^K l_k}{NKT}. \quad (22)$$

The interesting regime of parameters is:

$$1 \leq c \leq r \leq K, \quad (23a)$$

$$0 \leq L \leq 1 - \frac{r}{K}. \quad (23b)$$

Firstly, we argue that the regime of interest for L is $[0, 1 - r/K]$. By definition, $L \geq 0$. Moreover, each node k can trivially compute $|\mathcal{M}_k|$ of its desired IVAs locally and thus only needs to receive $N - |\mathcal{M}_k|$ IVAs from other nodes. Uncoded shuffling of these missing IVAs requires a communication load of $L = \frac{\sum_{k=1}^K (N - |\mathcal{M}_k|)T}{NKT} = 1 - \frac{r}{K}$. The question of interest is whether a coded shuffling procedure allows to reduce this communication load. Secondly, we argue that we can restrict attention to values of c and r satisfying (23a). Since each IVA needs to be computed at least once somewhere, we have $c \geq 1$. Moreover, the definition of \mathcal{C}_k in (14) implies that $|\mathcal{C}_k| \leq |\mathcal{M}_k|K$, and thus by (20) and (21) that $c \leq r$. Finally, the regime $r > K$ is not interesting, because in this case each node stores all the files, $\mathcal{M}_k = \{1, \dots, N\}$, and can thus locally compute all the IVAs required to compute its output function. In this case, $c \geq 1$ and $L \geq 0$ can be arbitrary.

Definition 4 (Fundamental SCC Region). *An SCC-triple (r, c, L) as in (23) is called feasible, if for any $\epsilon > 0$ and sufficient large N , there exist map, shuffle, and reduce procedures with storage space $r + \epsilon$, computation load $c + \epsilon$, and communication load $L + \epsilon$. The set of all feasible SCC triples \mathcal{R} is called the fundamental SCC region:*

$$\mathcal{R} \triangleq \{(r, c, L) : (r, c, L) \text{ is feasible}\}. \quad (24)$$

Definition 5 (Optimal Tradeoff Surface). *A SCC triple (r, c, L) is called pareto-optimal if it is feasible and if no feasible SCC triple (r', c', L') exists so that $r' \leq r$, $c' \leq c$ and $L' \leq L$ with one or more of the inequalities being strict. Define the optimal tradeoff surface as*

$$\mathcal{O} \triangleq \{(r, c, L) : (r, c, L) \text{ is pareto-optimal}\}. \quad (25)$$

The main objective of this paper is to identify the fundamental SCC region and its optimal tradeoff surface.

Remark 1. All our conclusions in this paper remain valid in an extended setup with Q output functions as in [3], where $K|Q$ and each node is supposed to compute $\frac{Q}{K}$ functions. In fact, in this setup, the K in definitions (21) and (22) will be replaced by Q . Achievability proofs can be shown by executing $\frac{Q}{K}$ times the distributed computing schemes as explained in Section IV and V. The converse can be derived by adjusting the definitions in (119), (121), (194), and following the same steps in Appendix B.

Remark 2. If each node k computes the IVAs required by all output functions from all files it stores, i.e.,

$$\mathcal{C}_k = \{v_{q,n} : q \in \mathcal{K}, w_n \in \mathcal{M}_k\}, \quad (26)$$

then $|\mathcal{C}_k| = |\mathcal{M}_k| \cdot K$, and the computation load becomes

$$c = \frac{\sum_{k=1}^K |\mathcal{C}_k|}{NK} \quad (27)$$

$$= \frac{\sum_{k=1}^K |\mathcal{M}_k| \cdot K}{NK} \quad (28)$$

$$= r. \quad (29)$$

This is exactly the case investigated in [3] where the fundamental storage-communication tradeoff is established.

This tradeoff is characterized by $L^*(r)$, which for integer values $r \in [K]$ is given by

$$L^*(r) \triangleq \frac{1}{r} \left(1 - \frac{r}{K}\right), \quad (30)$$

and for general r in the interval $[1, K]$ is given by

$$L^*(r) \triangleq \max_{i \in [K-1]} \left\{ -\frac{1}{i(i+1)}r + \frac{1}{i} + \frac{1}{i+1} - \frac{1}{K} \right\}. \quad (31)$$

III. THE FUNDAMENTAL SCC REGION AND OPTIMAL TRADEOFF SURFACE

In this section, we provide our main result on the fundamental SCC region. Proofs are deferred to Section IV and Appendix B and C.

Let us define the $2K - 1$ points $P_1, \dots, P_K, Q_2, \dots, Q_K$ in the storage-computation-communication space:

$$P_i \triangleq \left(i, i \left(1 - \frac{i-1}{K}\right), \frac{1}{i} \left(1 - \frac{i}{K}\right) \right), \quad i \in [K], \quad (32)$$

$$Q_i \triangleq \left(i, i, \frac{1}{i} \left(1 - \frac{i}{K}\right) \right), \quad i \in [2 : K]. \quad (33)$$

Notice that for each $i \in [2 : K]$,

$$Q_i = P_i + \frac{i(i-1)}{K} \cdot \vec{e}_2, \quad (34)$$

where $\vec{e}_2 \triangleq (0, 1, 0)$. Thus each of the lines $\overline{P_2Q_2}, \overline{P_3Q_3}, \dots, \overline{P_KQ_K}$ is parallel to \vec{e}_2 . Define now \mathcal{F} as the surface formed by the following triangles and trapezoids

$$\mathcal{F} \triangleq \{\triangle P_1P_2Q_2\} \cup \{\triangle P_{i-1}P_iP_K : i = 2, \dots, K-1\} \cup \{\square P_iQ_iQ_{i+1}P_{i+1} : i = 2, \dots, K-1\}. \quad (35)$$

It follows that the surface \mathcal{F} is connected and continuous. Further, we can show that it contains exactly one point (r, c, L) for each pair (r, c) satisfying (23a). This can be easily seen from Fig. 3, and is formally proved in Appendix A.

Theorem 1. *The fundamental SCC region \mathcal{R} is the set of SCC triples (r, c, L) satisfying (23) and lying on or above the surface \mathcal{F} , i.e.,*

$$\mathcal{R} = \{(r, c, L) : (r, c, L) \text{ is on or above the surface } \mathcal{F}\}. \quad (36)$$

Moreover, the optimal tradeoff surface \mathcal{O} is:

$$\mathcal{O} = \{\triangle P_{i-1}P_iP_K : i = 2, \dots, K-1\}. \quad (37)$$

An example of the fundamental SCC region for $K = 10$ is given in Fig. 3, where we can identify the surface \mathcal{F} that is formed by the triangles $\triangle P_1P_2Q_2$ and $\{\triangle P_{i-1}P_iP_K\}$ and the trapezoids $\{\square P_iQ_iQ_{i+1}P_{i+1}\}$.

In particular, the boundary of the optimal tradeoff surface \mathcal{O} is formed by the line segment $\overline{P_1P_K}$ and the sequence of line segments $\overline{P_1P_2}, \overline{P_2P_3}, \dots, \overline{P_{K-1}P_K}$:

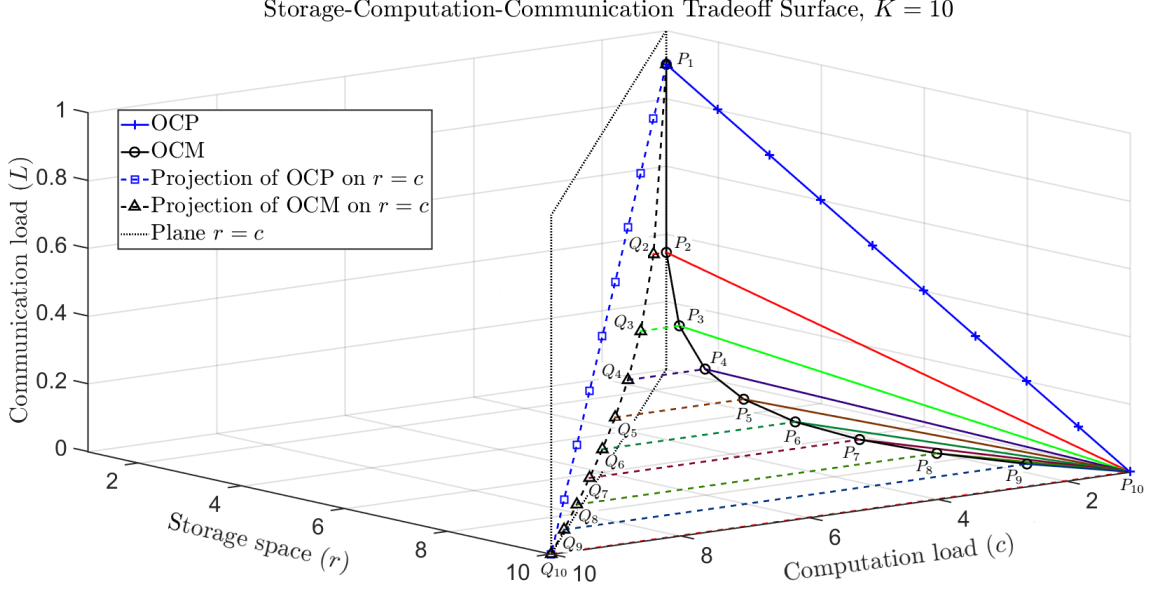


Fig. 3: The fundamental SCC region \mathcal{R} for a system with $K = 10$ nodes. The figure illustrates the delimiting surface \mathcal{F} formed by the triangles $\triangle P_1 P_2 Q_2$ and $\{\triangle P_{i-1} P_i P_K\}$ and the trapezoids $\{\square P_i Q_i Q_{i+1} P_{i+1}\}$.

- 1) The computation load on the line segment $\overline{P_1 P_K}$ is $c = 1$ for any given storage space r , which by (23) is minimal and thus is referred to as the *optimal computation curve (OCP)*. It implies that during the map phase each IVA is calculated at a single node. In other words, the points on $\overline{P_1 P_K}$ are achieved with an uncoded scheme.
- 2) The points on the line segments $\overline{P_1 P_2}$, $\overline{P_2 P_3}$, \dots , $\overline{P_{K-1} P_K}$ have minimum communication load L for any given storage space r among all pareto-optimal points, thus we refer to it as the *optimal communication curve (OCM)*. These points can be achieved by simply eliminating the redundancy in computation in CDC scheme (which will be referred to as the modified CDC (M-CDC) scheme, see Section IV).

Notice that the projections of OCP and OCM curves on the surface $r = c$ correspond to the curves of the uncoded scheme and the CDC scheme in [3] (See Fig. 2). In this sense, our optimal tradeoff surface \mathcal{O} is a natural extension of the tradeoff established in [3] with the additional dimension given by the computation load.

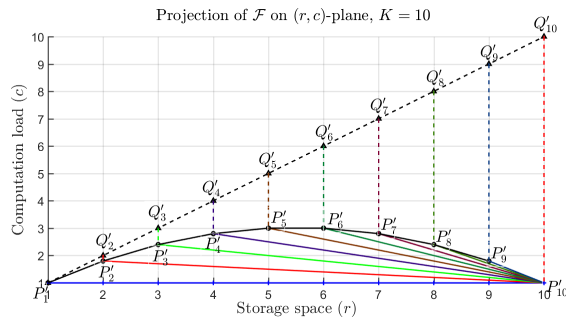


Fig. 4: Projection of the surface \mathcal{F} onto the (r, c) -plane. The points $P'_1, \dots, P'_{10}, Q'_2, \dots, Q'_{10}$ denote the projections of the points $P_1, \dots, P_{10}, Q_2, \dots, Q_{10}$.

Fig. 4 illustrates the projection of the surface \mathcal{F} onto the (r, c) -plane. The points P'_1, \dots, P'_{10} , indicate the projections of the optimal points P_1, \dots, P_{10} . We remark that when the available storage space exceeds a certain threshold, the necessary computation load is decreasing with the storage space. In fact, when storage space is large, each node can compute most of its desired IVAs locally, thus decreasing the number of IVAs a node has to compute for the coded shuffle phase. This effect however decreases the overall computation load, because coded shuffling requires that IVAs are calculated at two or more nodes.

Fig. 4 also shows the vertical gap between the line segments $\overline{P'_1 P'_2}, \overline{P'_2 P'_3}, \dots, \overline{P'_9 P'_{10}}$ and the line $r = c$, which includes the projections Q'_2, \dots, Q'_K of the points Q_2, \dots, Q_K attained by the original CDC scheme. This gap indicates the saving in computation load of the M-CDC scheme over the original CDC scheme. We notice that the savings increase as the storage space increases.

Finally, it is also interesting to consider the intersection between the optimal surface \mathcal{O} and a fixed communication-load plane or the intersection between \mathcal{O} and a fixed storage-space plane. An example for $K = 10$ is given in Fig. 5(a) for $L = 0.12$ and in Fig. 5(b) for $r = 4.5$, where the intersections are represented by the solid black lines. Fig. 5(a) shows that communication load $L = 0.12$ is possible for all (r, c) pairs that lie above the black line. Thus, when insisting on a given communication load, storage space can be traded for computation load and vice versa. The OCP point and the OCM point represent extreme points of minimum computation load or minimum required storage space. Analogous observations hold for Fig. 5(b).

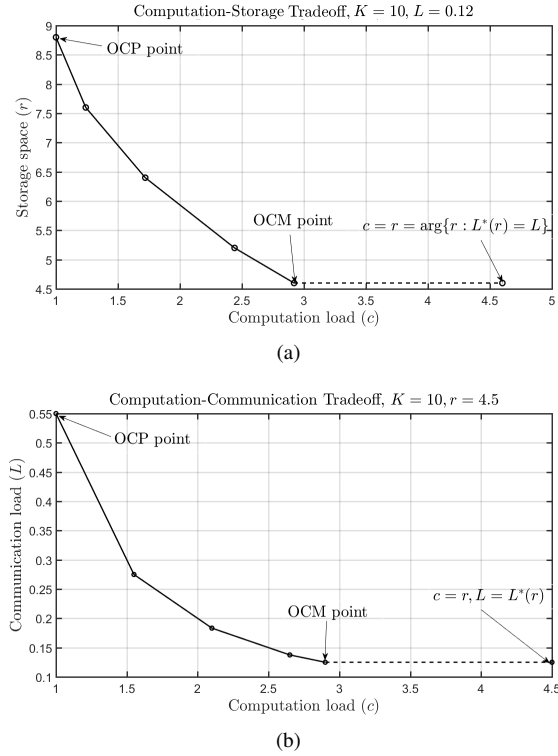


Fig. 5: Two-dimensional tradeoff curves for $K = 10$: (a) Computation-storage tradeoff with fixed communication load $L = 0.12$; (b) Computation-communication tradeoff with fixed storage space $r = 4.5$.

IV. MODIFIED CODED DISTRIBUTED COMPUTING (M-CDC)

In this section, we prove the achievability part of Theorem 1. Since in Appendix C we prove that the surface \mathcal{O} is the pareto-optimal tradeoff surface of the region \mathcal{R} , it suffices to show the achievability of all points on \mathcal{O} . As we shall explain shortly, the corner points P_1, P_2, \dots, P_K of the triangles forming \mathcal{O} are achieved by the M-CDC scheme proposed in [4]. For any other point P on $\triangle P_{i-1}P_iP_K$, there exists a unique triple $(\theta_1, \theta_2, \theta_3) \in [0, 1]^3$, such that $P = \theta_1 P_{i-1} + \theta_2 P_i + \theta_3 P_K$. Then P is achieved by dividing the N files into three groups of sizes² $\theta_1 N, \theta_2 N$ and $\theta_3 N$, and carrying out the M-CDC scheme achieving the points P_{i-1}, P_i and P_K for the three groups, respectively.

Before describing the M-CDC scheme in detail, we start with an illustrative example.

Example 1. Consider the computation task in Fig. 1, where $K = 3, N = 6$. Assume a storage space of $r = 2$. The M-CDC scheme is illustrated in Fig. 6. The top-most line in each of the three boxes indicates the files stored at the node. Below this line, is a rectangle indicating the map functions. The computed IVAs are depicted below the rectangle, where red circles indicate IVAs $\{v_{1,1}, \dots, v_{1,6}\}$, green squares IVAs $\{v_{2,1}, \dots, v_{2,6}\}$, and blue triangles IVAs $\{v_{3,1}, \dots, v_{3,6}\}$. The last line of each box indicates the IVAs that the node needs during the shuffle phase.

The dashed circles/squares/triangles stand for the IVAs that would be computed in addition in the CDC scheme, see [3, Example 1]. In other words, they represent the saving in computation load. In fact for this example, M-CDC and CDC have same communication load $L = \frac{1}{6}$, but different computation loads c . M-CDC has computation load $c = \frac{4}{3}$ and CDC has computation load $c = 2$.

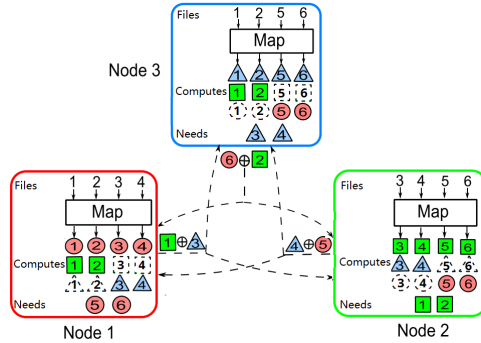


Fig. 6: An example of M-CDC scheme for a system with $K = 3$ nodes and $N = 6$ files.

We now describe the M-CDC scheme. The scheme is parametrized by the integer $i \in [K]$. For fixed i , the N files are partitioned into $\binom{K}{i}$ batches, each containing

$$\eta_i = \frac{N}{\binom{K}{i}} \quad (38)$$

²This requires that $\theta_1, \theta_2, \theta_3$ have to be rational. If any one is irrational, one can replace it by a rational number arbitrarily close to it.

files. Each batch is then associated with a subset \mathcal{T} of \mathcal{K} of cardinality i . Define

$$\Omega \triangleq \{\mathcal{T} \subseteq \mathcal{K} : |\mathcal{T}| = i\}, \quad (39)$$

and let $\mathcal{W}_{\mathcal{T}}$ denote the batch of the η_i files associated with set \mathcal{T} . Then,

$$\mathcal{W} = \{w_1, \dots, w_N\} = \bigcup_{\mathcal{T} \in \Omega} \mathcal{W}_{\mathcal{T}}. \quad (40)$$

Further let $\mathcal{U}_{\mathcal{T},k}$ be the set of IVAs for output function ϕ_k that can be computed from the files in $\mathcal{W}_{\mathcal{T}}$:

$$\mathcal{U}_{\mathcal{T},k} \triangleq \{v_{k,n} : w_n \in \mathcal{W}_{\mathcal{T}}\}. \quad (41)$$

We now describe the map, shuffle, and reduce procedures of the M-CDC scheme.

1) *Map Phase*: Each node k stores

$$\mathcal{M}_k = \bigcup_{\mathcal{T} \in \Omega: k \in \mathcal{T}} \mathcal{W}_{\mathcal{T}}, \quad (42)$$

and computes the IVAs

$$\mathcal{C}_k = \mathcal{C}_k^1 \cup \mathcal{C}_k^2, \quad (43)$$

where

$$\mathcal{C}_k^1 = \bigcup_{\mathcal{T} \in \Omega: k \in \mathcal{T}} \mathcal{U}_{\mathcal{T},k}, \quad (44)$$

$$\mathcal{C}_k^2 = \bigcup_{\mathcal{T} \in \Omega: k \in \mathcal{T}} \bigcup_{q \in \mathcal{K} \setminus \mathcal{T}} \mathcal{U}_{\mathcal{T},q}. \quad (45)$$

In other words, for each batch \mathcal{T} , each node k computes all the IVAs for its own function k , and all the IVAs for the function q if node q does not have the batch \mathcal{T} .

2) *Shuffle Phase*: For each element $\mathcal{T} \in \Omega$ and each index $j \in \mathcal{K} \setminus \mathcal{T}$, we partition the set $\mathcal{U}_{\mathcal{T},j}$ into i smaller subsets

$$\mathcal{U}_{\mathcal{T},j} = \{\mathcal{U}_{\mathcal{T},j}^k : k \in \mathcal{T}\} \quad (46)$$

of equal size. Define now the set

$$\Pi \triangleq \{\mathcal{S} \subseteq \mathcal{K} : |\mathcal{S}| = i + 1\}. \quad (47)$$

For each $\mathcal{S} \in \Pi$ and $k \in \mathcal{S}$, by (45), node k can compute the signal

$$X_{\mathcal{S}}^k \triangleq \bigoplus_{l \in \mathcal{S} \setminus \{k\}} \mathcal{U}_{\mathcal{S} \setminus \{l\},l}^k \quad (48)$$

from the IVAs calculated during the map phase. Node k thus sends the multicast signal

$$X_k = \{X_{\mathcal{S}}^k : \mathcal{S} \in \Pi \text{ such that } k \in \mathcal{S}\}. \quad (49)$$

- 3) *Reduce Phase*: Notice that \mathcal{C}_k^2 only contains the IVAs $v_{q,n}$ where $q \neq k$. Thus, by (43) and (44), during the shuffle phase each node k needs to learn all the IVAs in

$$\bigcup_{\mathcal{T} \in \Omega: k \notin \mathcal{T}} \mathcal{U}_{\mathcal{T},k}. \quad (50)$$

Fix an arbitrary $\mathcal{T} \in \Omega$ such that $k \notin \mathcal{T}$ and an element $j \in \mathcal{T}$. From the received multicast message

$$X_{\mathcal{T} \cup \{k\}}^j = \bigoplus_{l \in \mathcal{T} \cup \{k\} \setminus \{j\}} \mathcal{U}_{\mathcal{T} \cup \{k\} \setminus \{l\},l}^j \quad (51)$$

sent by node j during the shuffle phase and its locally calculated IVAs during the map phase

$$\left\{ \mathcal{U}_{\mathcal{T} \cup \{k\} \setminus \{l\},l}^j : l \in \mathcal{T} \setminus \{j\} \right\}, \quad (52)$$

node k can recover the missing IVA $\mathcal{U}_{\mathcal{T},k}^j$ through a simple XOR operation. Moreover, node k can decode $\mathcal{U}_{\mathcal{T},k}$ from

$$\left\{ X_{\mathcal{T} \cup \{k\}}^j : j \in \mathcal{T} \right\}. \quad (53)$$

After collecting all the missing IVAs, node k can proceed to compute the reduce function (19).

We analyze the performance of the scheme.

- 1) *Storage Space*: The number of batches in \mathcal{M}_k is $\binom{K-1}{i-1}$, each consisting of η_i files. Thus, the storage space is

$$r = \frac{1}{N} \cdot K \cdot \binom{K-1}{i-1} \cdot \eta_i = i. \quad (54)$$

- 2) *Computation Load*: Since $\mathcal{C}_k^1 \cap \mathcal{C}_k^2 = \emptyset$, we have $|\mathcal{C}_k| = |\mathcal{C}_k^1| + |\mathcal{C}_k^2|$. From (38), (44), and (45), we have

$$|\mathcal{C}_k^1| = \binom{K-1}{i-1} \cdot \eta_i = \frac{iN}{K}, \quad (55)$$

$$|\mathcal{C}_k^2| = \binom{K-1}{i-1} \cdot (K-i) \cdot \eta_i \quad (56)$$

$$= \left(1 - \frac{i}{K}\right) \cdot i \cdot N. \quad (57)$$

Thus, the computation load is

$$c = \frac{\sum_{k=1}^K |\mathcal{C}_k|}{NK} \quad (58)$$

$$= i \left(1 - \frac{i}{K}\right). \quad (59)$$

- 3) *Communication Load*: The number of signals that each node k transmits is $\binom{K-1}{i}$, each of size $\frac{\eta_i \cdot T}{i}$ bits. Thus, the length of the signal X_k is $l_k = \binom{K-1}{i} \frac{\eta_i \cdot T}{i}$ bits. Therefore, the communication load is

$$L = \frac{\sum_{k=1}^K l_k}{NKT} \quad (60)$$

$$= \frac{1}{i} \cdot \left(1 - \frac{i}{K}\right). \quad (61)$$

From (54), (59), and (61), we show the achievability of the SCC triple P_i .

Remark 3. In [33], we have proposed an alternative *distributed computing and coded communication (D3C)* scheme that achieves the same surface \mathcal{O} as the above scheme. The D3C scheme seems more involved. For example, to achieve a certain point in the interior of $\triangle P_{i-1}P_iP_K$, the D3C scheme may need to partition files into $\binom{K}{i}\binom{i}{g}$ batches, for some integer $g \geq 2$. In contrast, the time- and memory- sharing scheme described at the beginning of this subsection requires only $\binom{K}{i-1} + \binom{K}{i} + 1$ batches.

V. DISTRIBUTED COMPUTING SCHEMES WITH SMALL NUMBER OF FILES

Notice that, the M-CDC scheme requires at least $\binom{K}{i}$ files, which increases very fast in K . It is therefore not implementable in practice when there are many computing nodes. The goal of this section is to present distributed computing schemes that require only a small number of files N . For that purpose, we introduce placement delivery arrays.

A. Placement Delivery Arrays (PDA)

PDAs were introduced to conveniently represent placement and delivery of coded caching schemes with uncoded prefetching in a single array [31]. It was shown in [31] that any given PDA can be associated with a coded caching scheme for the shared-link model [30]. Several PDA constructions have been proposed in the literature, e.g., [31], [32], [34]. For completeness, we recall the definition of a PDA.

Definition 6 (Placement delivery array [31]). For positive integers K, F, Z and S , an $F \times K$ array $\mathbf{A} = [a_{i,j}]$, $i \in [F], j \in [K]$, composed of a specific symbol “*” and S ordinary symbols $1, \dots, S$, is called a (K, F, Z, S) *placement delivery array (PDA)*, if it satisfies the following conditions:

- C1. The symbol “*” appears Z times in each column;
- C2. Each ordinary symbol occurs at least once in the array;
- C3. For any two distinct entries a_{i_1, j_1} and a_{i_2, j_2} , we have $a_{i_1, j_1} = a_{i_2, j_2} = s$, an ordinary symbol only if
 - a. $i_1 \neq i_2, j_1 \neq j_2$, i.e., they lie in distinct rows and distinct columns; and
 - b. $a_{i_1, j_2} = a_{i_2, j_1} = *$, i.e., the corresponding 2×2 sub-array formed by rows i_1, i_2 and columns j_1, j_2 must be of the following form

$$\begin{bmatrix} s & * \\ * & s \end{bmatrix} \quad \text{or} \quad \begin{bmatrix} * & s \\ s & * \end{bmatrix}. \quad (62)$$

If each ordinary symbol $s \in [S]$ occurs exactly g times, \mathbf{A} is called a regular g -(K, F, Z, S) PDA, or g -PDA for short.

In these following subsections, we show that PDAs can also describe distributed computing schemes. We start by explaining the connection at hand of the previous Example 1.

B. PDA and Distributed Computing: Back to Example 1

Recall that Example 1 includes $K = 3$ nodes and $N = 6$ files, which are then partitioned into $F = 3$ batches:

$$\mathcal{W}_1 = \{w_1, w_2\}, \quad \mathcal{W}_2 = \{w_3, w_4\}, \quad \mathcal{W}_3 = \{w_5, w_6\}. \quad (63)$$

The coded distributed computing scheme of Example 1 is described by the following 3-(3, 3, 2, 1) PDA:

$$\mathbf{A} = \begin{bmatrix} * & 1 & * \\ * & * & 1 \\ 1 & * & * \end{bmatrix}. \quad (64)$$

So, \mathbf{A} has $F = 3$ rows (one for each batch) and $K = 3$ columns (one for each node). The “*”-symbols in the PDA describe the storage operations. Each node stores all the files of the batches that have a “*”-symbol in the corresponding column. For example, node 1, which is associated with the first column of the PDA, stores the files in batches \mathcal{W}_1 and \mathcal{W}_2 , because they are associated with the first two rows. Node 2, which is associated with the second column, stores the files in batches \mathcal{W}_2 and \mathcal{W}_3 , and node 3, which is associated with the third column, stores the files in batches \mathcal{W}_1 and \mathcal{W}_3 .

The ordinary symbols in the PDA describe the shuffling operations. And indirectly also some of the computations of IVAs during the map phase. In fact, during the map phase, each node first computes all its desired IVAs which it can obtain from its locally stored batches. Then, it also computes all IVAs that it is supposed to share during the shuffle phase. Specifically, in Example 1, node 1 first computes the circle IVAs of files 1, 2, 3, 4 pertaining to batches \mathcal{W}_1 and \mathcal{W}_2 ; node 2 first computes the square IVAs of files 3, 4, 5, 6 pertaining to batches \mathcal{W}_2 and \mathcal{W}_3 ; and node 3 first computes the triangle IVAs of files 1, 2, 5, 6 pertaining to batches \mathcal{W}_1 and \mathcal{W}_3 . Then, they also compute the IVAs needed to form the XOR messages exchanged in the shuffle phase.

These XOR messages are described by the ordinary symbol 1 in the PDA \mathbf{A} . Each node considers the subarray of \mathbf{A} that is formed by the columns associated with the other two nodes, and sends the XOR packet that the ordinary symbol 1 indicates for this subarray. For example, node 1 considers the subarray formed by the second and third columns of \mathbf{A} , where the ordinary symbol 1 appears in the first row of the second column and in the second row of the third column. These positions indicate that node 1 should multicast the XOR of a square IVA (i.e., an IVA for node 2) that can be computed from batch \mathcal{W}_1 and a triangle IVA (i.e., an IVA for node 3) that can be computed from batch \mathcal{W}_2 . Node 1 can compute both of these IVAs because it has stored both batches. In fact, column 1 has a “*”-symbol in the first and second row. We can verify that in Example 1, node 1 indeed sends the XOR between square IVA 1 and triangle IVA 3. From the described XOR, node 2 can recover its desired square IVA, because it can compute the triangle IVA locally (it has stored batch \mathcal{W}_1), and node 3 can recover its desired triangle IVA, because it can compute the square IVA locally (it has stored batch \mathcal{W}_1).

To create their own multicast messages for the shuffle phase, nodes 2 and 3 consider the subarrays of \mathbf{A} formed by the first and third columns, and by the first and second columns, respectively. The positions of the symbol 1 in these subarrays indicate that node 2 should multicast the XOR of a circle IVA (an IVA for node 1) that can be computed from batch \mathcal{W}_3 and of a triangle IVA (an IVA for node 3) that can be computed from batch \mathcal{W}_2 .

Similarly, node 3 should multicast the XOR of a circle IVA (an IVA for node 1) that can be computed from \mathcal{W}_3 and of a square IVA (an IVA for node 2) that can be computed from \mathcal{W}_1 . We can verify again that in Example 1, node 2 and node 3 indeed multicast the described XOR messages. Moreover, given the signals they sent and the IVAs they computed locally, node 1 can recover all the circle IVAs, node 2 can recover all square IVAs, and node 3 can recover all triangle IVAs.

Each node k then terminates the reduce phase by applying the reduce function h_k to all its recovered IVAs.

Remark 4. As we have seen, an ordinary symbol that occurs g times in the PDA, describes g different multicast messages sent by g different nodes. Each multicast message is useful for $g - 1$ nodes, and thus has coding gain $g - 1$. In the shared-link caching scenario [30], a single ordinary symbol describes the transmission of a *single* multicast message from the server to g different nodes. Each multicast message is thus useful for g nodes, and thus has coding gain g .

C. Distributed Computing Schemes from PDAs

In this section, we explain how to obtain a distributed computing scheme from any (K, F, Z, S) PDA where each ordinary symbol occurs at least twice.

Consider a (K, F, Z, S) PDA $\mathbf{A} = [a_{i,j}]$, such that each ordinary symbol in $[S]$ occurs twice or more. Partition the N files into F batches $\mathcal{W}_1, \dots, \mathcal{W}_F$, each containing

$$\eta \triangleq \frac{N}{F} \quad (65)$$

files. Then,

$$\mathcal{W} = \{w_1, \dots, w_N\} = \bigcup_{i \in [F]} \mathcal{W}_i. \quad (66)$$

Further, let $\mathcal{U}_{i,j}$ be the set of IVAs for the output function ϕ_j that can be computed from the files in \mathcal{W}_i , i.e.,

$$\mathcal{U}_{i,j} \triangleq \{v_{j,n} : w_n \in \mathcal{W}_i\}, \quad (67)$$

and let \mathcal{A}_k denote the set of ordinary symbols in column k :

$$\mathcal{A}_k \triangleq \{s \in [S] : a_{i,k} = s \text{ for some } i \in [F]\}, \quad k \in [K]. \quad (68)$$

1) *Map Phase:* Each node k stores

$$\mathcal{M}_k = \bigcup_{\substack{i \in [F]: \\ a_{i,k} = *}} \mathcal{W}_i, \quad (69)$$

and computes the IVAs

$$\mathcal{C}_k = \mathcal{C}_k^{(1)} \cup \mathcal{C}_k^{(2)}, \quad (70)$$

where

$$\mathcal{C}_k^{(1)} = \bigcup_{\substack{i \in [F]: \\ a_{i,k} = *}} \mathcal{U}_{i,k}, \quad (71)$$

$$\mathcal{C}_k^{(2)} = \bigcup_{s \in \mathcal{A}_k} \bigcup_{\substack{(l,q) \in [F] \times ([K] \setminus \{k\}): \\ a_{l,q} = s}} \mathcal{U}_{l,q}. \quad (72)$$

Notice that node k can compute the IVAs in $\mathcal{C}_k^{(1)}$ from the files in \mathcal{M}_k , because of (67), (69), and (71). To show that it can also compute the IVAs in $\mathcal{C}_k^{(2)}$ from \mathcal{M}_k , we show that if for some $s \in \mathcal{A}_k$ there exist $(l, q) \in [F] \times ([K] \setminus \{k\})$ so that $a_{l,q} = s$, then

$$a_{l,k} = *. \quad (73)$$

From this follows that $\mathcal{W}_l \in \mathcal{M}_k$. To see (73), notice that by the definition of the set \mathcal{A}_k , there exists an index $i \in [F]$ so that $a_{i,k} = s$. But by the PDA property C3, $a_{l,q} = a_{i,k} = s$ and $q \neq k$ imply that $l \neq i$ and $a_{l,k} = a_{i,q} = *$.

- 2) *Shuffle Phase:* For each pair $(i, k) \in [F] \times [K]$ such that $a_{i,k} \neq *$ do the following. Set $s = a_{i,k}$, and let g_s denote the occurrence of the ordinary symbol s in \mathbf{A} . Partition the IVAs in $\mathcal{U}_{i,k}$ into $g_s - 1$ smaller blocks of equal size. Let $(l_1, j_1), (l_2, j_2), \dots, (l_{g_s-1}, j_{g_s-1})$ indicate all the other $g_s - 1$ occurrences of the ordinary symbol s other than (i, k) :

$$a_{l_1, j_1} = a_{l_2, j_2} = \dots = a_{l_{g_s-1}, j_{g_s-1}} = s. \quad (74)$$

We denote the $g_s - 1$ subblocks of $\mathcal{U}_{i,k}$ by $\mathcal{U}_{i,k}^{j_1}, \dots, \mathcal{U}_{i,k}^{j_{g_s-1}}$:

$$\mathcal{U}_{i,k} = \left\{ \mathcal{U}_{i,k}^{j_1}, \dots, \mathcal{U}_{i,k}^{j_{g_s-1}} \right\}. \quad (75)$$

Node $k \in \mathcal{K}$ then computes for each $s \in \mathcal{A}_k$:

$$X_s^k \triangleq \bigoplus_{\substack{(i,j) \in [F] \times ([K] \setminus \{k\}): \\ a_{i,j} = s}} \mathcal{U}_{i,j}^k \quad (76)$$

from \mathcal{C}_k , and multicasts the signal

$$X_k = \{X_s^k : s \in \mathcal{A}_k\}. \quad (77)$$

- 3) *Reduce Phase:* Node k has to compute all IVAs in

$$\bigcup_{i \in [F]} \mathcal{U}_{i,k}. \quad (78)$$

In the map phase, node k has already computed all IVAs in $\mathcal{C}_k^{(1)}$. It thus remains to compute all IVAs in

$$\bigcup_{\substack{i \in [F]: \\ a_{i,k} \neq *}} \mathcal{U}_{i,k}. \quad (79)$$

Fix an arbitrary $i \in [F]$ such that $a_{i,k} \neq *$. Set $s = a_{i,k}$. Each subset $\mathcal{U}_{i,k}^j$ in (75) can be restored by node k from the signal X_s^j sent by node j :

$$X_s^j = \bigoplus_{\substack{(l,q) \in [F] \times ([K] \setminus \{j\}): \\ a_{l,q} = s}} \mathcal{U}_{l,q}^j. \quad (80)$$

In fact, for each $\mathcal{U}_{l,q}^j$ in (80), if $q \neq k$, then $a_{l,q} = a_{i,k} = s \in \mathcal{A}_k$. This indicates that, the IVAs in $\mathcal{U}_{l,q}^j$ have been computed by node k according to (72) and (75). If $q = k$, then $a_{l,q} = a_{i,k} = s$ implies $l = i$ by the PDA property C3-a. Therefore, $\mathcal{U}_{i,k}^j$ can be decoded from (80).

Let us now analyze the performance of the proposed scheme.

- 1) *Storage Space*: From (69) and the fact that each column of \mathbf{A} has Z occurrences of the “*” symbol, each node stores Z batches of files, i.e., $|\mathcal{M}_k| = Z\eta$. The storage space is thus:

$$r_{\mathbf{A}} = \frac{\sum_{k=1}^K |\mathcal{M}_k|}{N} = \frac{KZ}{F}. \quad (81)$$

- 2) *Computation Load*: Since $\mathcal{C}_k^{(1)} \cap \mathcal{C}_k^{(2)} = \emptyset$, we have $|\mathcal{C}_k| = |\mathcal{C}_k^{(1)}| + |\mathcal{C}_k^{(2)}|$. From (71) and (72),

$$|\mathcal{C}_k^{(1)}| = Z \cdot \eta, \quad (82)$$

$$|\mathcal{C}_k^{(2)}| = \sum_{s \in \mathcal{A}_k} (g_s - 1) \cdot \eta. \quad (83)$$

where g_s is the occurrence of the symbol s . Thus, the computation load is

$$c_{\mathbf{A}} = \frac{\sum_{k=1}^K |\mathcal{C}_k|}{NK} \quad (84)$$

$$= \frac{\sum_{k=1}^K Z \cdot \eta + \sum_{k=1}^K \sum_{s \in \mathcal{A}_k} (g_s - 1) \cdot \eta}{NK} \quad (85)$$

$$= \frac{Z}{F} + \sum_{k=1}^K \sum_{s \in \mathcal{A}_k} \frac{g_s - 1}{KF} \quad (86)$$

$$= \frac{Z}{F} + \sum_{s \in [S]} \frac{g_s(g_s - 1)}{KF}. \quad (87)$$

Denote the number of ordinary symbols having occurrence t by S_t ($t \in [2 : K]$), and define the fraction of the non-“*” entries having occurrence t in \mathbf{A} by

$$\theta_t \triangleq \frac{S_t t}{K(F - Z)}. \quad (88)$$

Then by (87),

$$\begin{aligned} c_{\mathbf{A}} &= \frac{Z}{F} + \sum_{t=2}^K \frac{S_t t(t-1)}{KF} \\ &= \frac{Z}{F} + \sum_{t=2}^K \frac{S_t t}{K(F-Z)} \cdot \frac{K(F-Z)}{KF} \cdot (t-1) \end{aligned} \quad (89)$$

$$= \frac{Z}{F} + \sum_{t=2}^K \theta_t \left(1 - \frac{Z}{F}\right) (t-1). \quad (90)$$

3) *Communication Load*: From (76), for each $s \in \mathcal{A}_k$, node k sends a signal of length $\frac{\eta \cdot T}{g_s - 1}$ bits. Therefore, the total length of the signal X_k is $l_k = \sum_{s \in \mathcal{A}_k} \frac{\eta \cdot T}{g_s - 1}$, and the communication load is

$$L_{\mathbf{A}} = \frac{\sum_{k=1}^K l_k}{NKT} \quad (91)$$

$$= \sum_{k=1}^K \sum_{s \in \mathcal{A}_k} \frac{1}{NKT} \cdot \frac{\eta \cdot T}{g_s - 1} \quad (92)$$

$$= \sum_{s \in [S]} \frac{g_s}{g_s - 1} \cdot \frac{1}{KF} \quad (93)$$

$$= \sum_{t=2}^K \frac{S_t t}{t-1} \cdot \frac{1}{KF} \quad (94)$$

$$= \sum_{t=2}^K \frac{S_t t}{K(F-Z)} \cdot \frac{1}{t-1} \cdot \frac{K(F-Z)}{KF} \quad (95)$$

$$= \sum_{t=2}^K \frac{\theta_t}{t-1} \left(1 - \frac{Z}{F}\right). \quad (96)$$

We summarize the above analysis with the following theorem.

Theorem 2. *For any given (K, F, Z, S) PDA \mathbf{A} , with each ordinary symbol occurring at least twice, let θ_t denote the fraction of non-“*” entries occurring t times, then there exists a distributed computing scheme that achieves the SCC triple*

$$(r_{\mathbf{A}}, c_{\mathbf{A}}, L_{\mathbf{A}}) = \left(\frac{KZ}{F}, \frac{Z}{F} + \sum_{t=2}^K \theta_t \left(1 - \frac{Z}{F}\right) (t-1), \sum_{t=2}^K \frac{\theta_t}{t-1} \left(1 - \frac{Z}{F}\right) \right). \quad (97)$$

The smallest number of files required to implement the scheme is F .

D. PDAs Achieving the Optimal Tradeoff Surface

Naturally, we are interested in identifying the PDAs whose associated distributed computing schemes achieve points on the optimal tradeoff surface. The following theorem addresses this problem. It is proved in Appendix D.

Theorem 3. *Given a (K, F, Z, S) PDA \mathbf{A} , with each ordinary symbol occurring at least twice. The distributed computing scheme associated to \mathbf{A} achieves the optimal tradeoff surface \mathcal{O} if, and only if, all ordinary symbols occur either g or $g+1$ times, for some $g \in \{2, 3, \dots, K-1\}$.*

Assume now that each ordinary symbol of \mathbf{A} occurs either g or $g+1$ times, for some $g \in \{2, 3, \dots, K-1\}$. The distributed computing scheme associated with \mathbf{A} achieves the pareto-optimal SCC triple

$$(r_{\mathbf{A}}, c_{\mathbf{A}}, L_{\mathbf{A}}) = \left(\frac{KZ}{F}, \frac{Z}{F} + \left(1 - \frac{Z}{F}\right)(g - \theta), \frac{g-1+\theta}{g(g-1)} \left(1 - \frac{Z}{F}\right) \right), \quad (98)$$

where $\theta \triangleq \frac{Sg(g+1)}{K(F-Z)} - g$, is the fraction of non-“*” entries occurring g times. The triple lies on the triangle $\triangle P_{g-1}P_gP_K$.

Example 2. The following is a $(5, 4, 2, 4)$ PDA, where the ordinary symbols 2, 3 occur twice, and 1, 4 occur three times.

$$\begin{bmatrix} * & 1 & * & 4 & * \\ * & 2 & 3 & * & 4 \\ 3 & * & * & 2 & 1 \\ 4 & * & 1 & * & * \end{bmatrix}. \quad (99)$$

According to Theorem 3, $\theta = \frac{2}{5}$, and it achieves the pareto-optimal SCC triple $(\frac{5}{2}, \frac{13}{10}, \frac{7}{20})$ for a system with 5 computing nodes.

Theorem 3 shows that, *almost-regular* PDAs where all non-“*” symbols occur g or $g+1$ times give pareto-optimal SCC triples. For g -regular PDAs with $g \geq 2$, we obtain:

Corollary 1. For any g -regular (K, F, Z, S) PDA \mathbf{A} , where $2 \leq g \leq K$, the associated distributed computing scheme achieves the pareto-optimal SCC triple

$$(r_{\mathbf{A}}, c_{\mathbf{A}}, L_{\mathbf{A}}) = \left(\frac{KZ}{F}, \frac{Z}{F} + \left(1 - \frac{Z}{F}\right)(g-1), \frac{1}{g-1} \left(1 - \frac{Z}{F}\right) \right), \quad (100)$$

which lies on the line segment $\overline{P_{g-1}P_K}$.

Proof. For a g -regular PDA, all non-“*” entries have g occurrences, thus (100) is obtained by setting $\theta = 1$ in (98) when $g \in [2 : K-1]$ and setting $\theta = 0, g = K-1$ in (98) when $g = K$. It remains to show that the SCC triple in (100) actually lies on the line segment $\overline{P_{g-1}P_K}$. By the definitions of the points P_{g-1} and P_K in (32), a point (r, c, L) is on this line if, and only if,

$$\frac{r-K}{(g-1)-K} = \frac{c-1}{(g-1)\left(1-\frac{g-2}{K}\right)-1} = \frac{L}{\frac{1}{g-1}\left(1-\frac{g-1}{K}\right)}, \quad (101)$$

which holds for the point $(r_{\mathbf{A}}, c_{\mathbf{A}}, L_{\mathbf{A}})$ in (100). Since $(r_{\mathbf{A}}, c_{\mathbf{A}}, L_{\mathbf{A}})$ is on the triangle $\triangle P_{g-1}P_gP_K$, by Theorem 3, we conclude that it is on the line segment $\overline{P_{g-1}P_K}$. \square

Remark 5. Corollary 1 indicates that, a distributed computing scheme associated with a $(i+1)$ - $\left(K, \binom{K}{i}, \binom{K-1}{i-1}, \binom{K}{i+1}\right)$ PDA achieves the SCC triple P_i , where $i \in [K-1]$. It is shown in [31] that, such a PDA can be constructed by the Maddah-Ali and Niesen coded caching scheme [30]. Thus, it corresponds to the M-CDC scheme.

Corollary 1 is of particular interest since there are several explicit regular PDA constructions for coded caching

in the literature, such as [31], [32]. The PDA constructions in [31] can decrease the subpacketization level of the coded caching scheme by a factor that increases exponentially with the number of users, while suffering only a slight loss in rate. The constructions in [32] work with a subpacketization level that only increases sub-exponentially with the number of users. In the following, we analyze the performances of these PDA constructions when they are applied to distributed computing.

E. Coded Computing Schemes from Existing PDAs

1) *Constructions from [31]*: Two classes of PDAs from [31, Theorems 4 and 5] have been proved useful to derive coded caching schemes with low subpacketization levels for the shared-link model. We use the same PDA constructions to obtain distributed computing schemes that work with only a small number of files. In [31] it is shown that for each $q|K$, where $1 < q < K$ and, $m = \frac{K}{q}$, there exist

- 1) a m -($qm, q^{m-1}, q^{m-2}, q^m - q^{m-1}$) PDA; and
- 2) a $(q-1)m$ -($qm, (q-1)q^{m-1}, (q-1)^2q^{m-2}, q^{m-1}$) PDA.

By Corollary 1, we then have the following.

Corollary 2. *For any integer $q|K$ with $1 < q < K$,*

- 1) *the pareto-optimal SCC triple*

$$D_{1,q} \triangleq \left(\frac{K}{q}, \frac{K(q-1)}{q^2} - \frac{q-2}{q}, \frac{q-1}{K-q} \right) \quad (102)$$

is achievable when the number of files is a multiple of $q^{\frac{K}{q}-1}$;

- 2) *the pareto-optimal SCC triple*

$$D_{2,q} \triangleq \left(\frac{K(q-1)}{q}, \frac{K(q-1)}{q^2} + \frac{q-2}{q}, \frac{1}{K(q-1)-q} \right) \quad (103)$$

is achievable when the number of files is a multiple of $(q-1)q^{\frac{K}{q}-1}$.

Proof: Notice that for the first PDA construction,

$$\frac{Z}{F} = \frac{1}{q} \quad \text{and} \quad g = \frac{K}{q}. \quad (104)$$

Plugging these values into the right-hand side of (100) in Corollary 1, results in $D_{1,q}$.

For the second PDA construction,

$$\frac{Z}{F} = \frac{q-1}{q} \quad \text{and} \quad g = \frac{K(q-1)}{q}, \quad (105)$$

and thus (100) evaluates to $D_{2,q}$. ■

We fix q and compare the two SCC triples $D_{1,q}$ and $D_{2,q}$ with the SCC triples

$$P_{\frac{K}{q}-1} = \left(\frac{K}{q} - 1, \frac{K(q-1)}{q^2} - \frac{q-3}{q} - \frac{2}{K}, \frac{q-1+q/K}{K-q} \right), \quad (106)$$

$$P_{\frac{K(q-1)}{q}-1} = \left(\frac{K(q-1)}{q} - 1, \frac{K(q-1)}{q^2} + \frac{2q-3}{q} - \frac{2}{K}, \frac{1+q/K}{K(q-1)-q} \right). \quad (107)$$

TABLE I: The asymptotic comparison between M-CDC scheme and Corollary 2.

ratio	storage	computation	communication	number of files
$P_{\frac{K}{q}-1}$ vs. $D_{1,q}$	$\lesssim 1$	$\gtrsim 1$	$\gtrsim 1$	$\sim \frac{q^2}{\sqrt{2\pi K}(q-1)^{\frac{3}{2}}} e^{K(1-\frac{1}{q}) \ln \frac{q}{q-1}}$
$P_{\frac{K(q-1)}{q}-1}$ vs. $D_{2,q}$	$\lesssim 1$	$\gtrsim 1$	$\gtrsim 1$	$\sim \frac{q^2}{\sqrt{2\pi K}(q-1)^{\frac{3}{2}}} e^{K(1-\frac{1}{q}) \ln \frac{q}{q-1}}$

One observes that $D_{1,q}$ and $D_{2,q}$ have slightly smaller computation and communication loads than $P_{\frac{K}{q}-1}$ and $P_{\frac{K(q-1)}{q}-1}$, but they require slightly larger storage spaces. In the asymptotic regime where $K \rightarrow \infty$, the three ratios obtained by dividing computation load, communication load, or storage space of $D_{1,q}$ by the ones of $P_{\frac{K}{q}-1}$, all tend to 1. The same applies also for the points $D_{2,q}$ and $P_{\frac{K(q-1)}{q}-1}$. However, the M-CDC scheme requires at least

$$\left(\frac{K}{\frac{K}{q}-1} \right) = \frac{K}{K(q-1)+q} \cdot \left(\frac{K}{\frac{K}{q}} \right) \sim \frac{q}{\sqrt{2\pi K}(q-1)^{\frac{3}{2}}} e^{K(\frac{1}{q} \ln q + (1-\frac{1}{q}) \ln \frac{q}{q-1})} \quad (108a)$$

files to achieve the point $P_{\frac{K}{q}-1}$, and it requires at least

$$\left(\frac{K}{\frac{K(q-1)}{q}-1} \right) = \frac{K+q}{K(q-1)} \cdot \left(\frac{K}{\frac{K(q-1)}{q}} \right) \sim \frac{q}{\sqrt{2\pi K}(q-1)^{\frac{3}{2}}} e^{K(\frac{1}{q} \ln q + (1-\frac{1}{q}) \ln \frac{q}{q-1})} \quad (108b)$$

files to achieve the point $P_{\frac{K(q-1)}{q}-1}$. The approximations on the right-hand sides of (108) hold in the asymptotic regime $K \rightarrow \infty$ and are from [31, Lemma 4]. Comparing (108) with Corollary 2 shows that the minimum number of files required to attain $D_{1,q}$ and $D_{2,q}$ is exponentially smaller in K than the number of files the M-CDC scheme needs to achieve the points $P_{\frac{K}{q}-1}$ and $P_{\frac{K(q-1)}{q}-1}$. Table I summarizes these comparisons of the points $D_{1,q}$, $P_{\frac{K}{q}-1}$ and the points $D_{2,q}$, $P_{\frac{K(q-1)}{q}-1}$. The sign \gtrsim (resp. \lesssim) indicates that for any finite K the ratio is larger (resp. smaller) than 1 but that in the asymptotic regime $K \rightarrow \infty$ it tends to 1.

2) *Constructions from [32]:* For any positive integers q, m, t such that $q \geq 2, 0 < t < m$, there exists PDAs with the following parameters:

- 1) a $\binom{m}{t} - \binom{m}{t} q^t, q^m, q^m - q^{m-t}(q-1)^t, q^m(q-1)^t$ PDA; and
- 2) a $\binom{m}{t}(q-1)^t - \binom{m}{t} q^t, q^m(q-1)^t, q^m(q-1)^t - q^{m-t}(q-1)^t, q^m$.

Corollary 3. For a distributed computing system with $K = \binom{m}{t} q^t$ nodes, where $q, m, t \in \mathbb{N}^+$ satisfying $q \geq 2, 0 < t < m$,

- 1) the parato-optimal SCC triple

$$E_{1,q,t} = \left(K \left(1 - \left(1 - \frac{1}{q} \right)^t \right), 1 + \frac{K}{q^t} \left(1 - \frac{1}{q} \right)^t - 2 \left(1 - \frac{1}{q} \right)^t, \frac{(q-1)^t}{K - q^t} \right) \quad (109)$$

is achievable when the number of files is a multiple of q^m .

- 2) the parato-optimal SCC triple

$$E_{2,q,t} = \left(K \left(1 - \frac{1}{q^t} \right), 1 + \frac{K}{q^t} \left(1 - \frac{1}{q} \right)^t - \frac{2}{q^t}, \frac{1}{K(q-1)^t - q^t} \right) \quad (110)$$

is achievable when the number of files is a multiple of $q^m(q-1)^t$.

Proof: Notice that for the first PDA construction,

$$\frac{Z}{F} = 1 - \left(1 - \frac{1}{q}\right)^t \quad \text{and} \quad g = \frac{K}{q^t}. \quad (111)$$

Plugging these values into the right-hand side of (100) in Corollary 1, we obtain $E_{1,q,t}$.

Similarly, with the second PDA construction,

$$\frac{Z}{F} = 1 - \frac{1}{q^t} \quad \text{and} \quad g = K \left(1 - \frac{1}{q}\right)^t, \quad (112)$$

and thus (100) leads to $E_{2,q,t}$. ■

If $t = 1$, then $E_{1,q,t}$ (resp. $E_{2,q,t}$) coincides with $D_{1,q}$ (resp. $D_{2,q}$). However, the required number of files in Corollary 3 is q times larger than that in Corollary 2.

The more interesting case is when $t \geq 2$. Generally, the scheme supports a large number of nodes $K = \binom{m}{t} q^t$. By Corollary 1, the SCC triple $E_{1,q,t}$ (resp. $E_{2,q,t}$) is on the line segment $\overline{P_{\frac{K}{q^t}-1} P_K}$ (resp. $\overline{P_{K(\frac{q-1}{q})^t-1} P_K}$). From Corollary 3, the number of files q^m (resp. $q^m(q-1)^t$) suffices to achieve $E_{1,q,t}$ (resp. $E_{2,q,t}$). By the inequality $\left(\frac{m}{t}\right)^t < \binom{m}{t} < \left(\frac{me}{t}\right)^t$, we have $\frac{tK^{\frac{1}{t}}}{eq} < m < \frac{tK^{\frac{1}{t}}}{q}$. Thus, the required number of files is

$$q^{\Theta\left(\frac{tK^{\frac{1}{t}}}{q}\right)} \left(\text{resp. } (q-1)^t q^{\Theta\left(\frac{tK^{\frac{1}{t}}}{q}\right)} \right), \quad (113)$$

which increases sub-exponentially with the number of nodes K . Recall that, SCC triple $E_{1,q,t}$ (resp. $E_{2,q,t}$) can also be achieved by time- and memory- sharing the M-CDC scheme achieving the points $P_{\frac{K}{q^t}-1}$ (resp. $P_{K(\frac{q-1}{q})^t-1}$) and P_K , where the required number of files at the points $P_{\frac{K}{q^t}-1}$ (resp. $P_{K(\frac{q-1}{q})^t-1}$) is

$$\left(\frac{K}{q^t} - 1\right) \left(\text{resp. } \left(K \left(\frac{q-1}{q}\right)^t - 1\right) \right). \quad (114)$$

For instance, for a system with $K = 180$ nodes, let $q = 2, t = 2, m = 10$. Then Corollary 3 indicates that $E_{1,q,t}$ can be achieved with 1024 input files, while the M-CDC scheme achieving $P_{\frac{K}{q^t}-1}$ requires $\binom{180}{44} \approx 2 \times 10^{42}$ files.

VI. CONCLUSION

We characterized the fundamental storage-computation-communication tradeoff region of the MapReduce framework and the corresponding pareto-optimal surface. Achievability of the fundamental tradeoff region is attained by time- and memory- sharing different points achieved by the M-CDC scheme. This scheme is similar to the original CDC scheme, but eliminates the redundant computations. An information-theoretical converse is also provided.

A major disadvantage of the M-CDC scheme (and the CDC scheme) is that the required number of input files N grows very fast in the number of nodes K . In this work, we provided new distributed computing schemes that also achieve points on the pareto-optimal tradeoff surface, but require an exponentially smaller (in K) number of files than the M-CDC scheme. To obtain these new schemes, we proceeded in three steps. We first showed that placement delivery array (PDA), a tool introduced for coded caching, can be used to describe a distributed

computing scheme. Then we characterized all PDAs that achieve points on the optimal tradeoff surface. Finally, we used existing regular PDA constructions with low subpacketization level from coded caching, to obtain the desired distributed computing schemes that work for small numbers of files.

ACKNOWLEDGEMENT

The work of Q. Yan and M. Wigger has been supported by the ERC under grant agreement 715111.

APPENDIX A

PROOF OF PROPERTIES OF SURFACE \mathcal{F}

That \mathcal{F} is connected and continuous, follows simply because it can be obtained by successively pasting a triangle or a trapezoid to the boundary of the previously obtained region.

We turn to prove that for each pair (r, c) satisfying (23a), there exists exactly one point $(r, c, L) \in \mathcal{F}$. That there exists *at least one* such point follows by the continuity of \mathcal{F} and because the triangle obtained by projecting the line segments $\overline{P_1Q_2}, \overline{Q_2Q_3}, \overline{Q_3Q_4}, \overline{Q_4Q_5}, \dots, \overline{Q_{K-1}Q_K}, \overline{Q_KP_K}, \overline{P_KP_1}$ onto the (r, c) -plane, contains all extreme points (r, c) that satisfy (23a). On the other hand, for each (r, c) there is not more than one point $(r, c, L) \in \mathcal{F}$, because none of the triangles and trapezoids that build \mathcal{F} is vertical and the projections of any two facets in \mathcal{F} onto the (r, c) -plane have non-overlap interiors.

APPENDIX B

PROOF OF THE CONVERSE IN THEOREM 1

A. Converse

Fix a map-shuffle-reduce procedure, and let $\mathcal{M} = \{\mathcal{M}_k\}_{k=1}^K, \mathcal{C} = \{\mathcal{C}_k\}_{k=1}^K$ be their file and IVA allocation. Let further (r, c, L) denote the corresponding storage space, computation load, and communication load, then

$$r = \frac{\sum_{k=1}^K |\mathcal{M}_k|}{N}, \quad (115)$$

$$c = \frac{\sum_{k=1}^K |\mathcal{C}_k|}{NK}, \quad (116)$$

$$L \geq \frac{\sum_{k=1}^K H(X_k)}{NKT}. \quad (117)$$

For any nonempty set $\mathcal{S} \subseteq \mathcal{K}$, denote

$$X_{\mathcal{S}} \triangleq \bigcup_{k \in \mathcal{S}} \{X_k\}, \quad (118)$$

$$\mathcal{V}_{\mathcal{S}} \triangleq \bigcup_{k \in \mathcal{S}} \mathcal{V}_k, \quad (119)$$

$$\mathcal{C}_{\mathcal{S}} \triangleq \bigcup_{k \in \mathcal{S}} \mathcal{C}_k. \quad (120)$$

For any $k \in \mathcal{S}, j \in [|\mathcal{S}| - 1]$, define

$$\mathcal{B}_{\mathcal{S},j}^k \triangleq \{v_{k,n} : v_{k,n} \text{ is only computed by } j \text{ nodes in } \mathcal{S} \setminus \{k\}\}. \quad (121)$$

Let $b_{S,j}^k$ be the cardinality of $\mathcal{B}_{S,j}^k$. Then it follows that the cardinality of

$$\mathcal{B}_{S,j} \triangleq \bigcup_{k \in \mathcal{S}} \mathcal{B}_{S,j}^k \quad (122)$$

is

$$b_{S,j} \triangleq |\mathcal{B}_{S,j}| = \sum_{k \in \mathcal{S}} b_{S,j}^k. \quad (123)$$

To prove the converse, we need the following two lemmas, the proofs of which are deferred to the following two subsections.

Lemma 1. For any nonempty set $\mathcal{S} \subseteq \mathcal{K}$ and $\mathcal{S}^c \triangleq \mathcal{K} \setminus \mathcal{S}$,

$$H(X_{\mathcal{S}} | \mathcal{V}_{\mathcal{S}^c}, \mathcal{C}_{\mathcal{S}^c}) \geq T \sum_{j=1}^{|\mathcal{S}|-1} b_{S,j} \cdot \frac{1}{j}. \quad (124)$$

Lemma 2. In (122) and (123), let $b_j \triangleq b_{\mathcal{K},j}$ be the cardinality of the set in (122) when $\mathcal{S} = \mathcal{K}$. Then

$$\sum_{j=1}^{K-1} b_j \geq N(K-r), \quad (125)$$

$$\sum_{j=1}^{K-1} (j-1)b_j \leq (c-1)NK. \quad (126)$$

Now, let us define, for each $i \in [K]$,

$$c_i = \frac{r}{K} + \left(1 - \frac{r}{K}\right) i, \quad (127)$$

and let for a fixed $i \in \{2, \dots, K-1\}$, the parameters $\lambda_i, \mu_i \in \mathbb{R}^+$ be such that

$$\lambda_i x + \mu_i |_{x=c_{i-1}} = \frac{1}{c_{i-1} - r/K} \left(1 - \frac{r}{K}\right)^2 \quad (128)$$

$$= \frac{1}{i-1} \left(1 - \frac{r}{K}\right), \quad (129)$$

$$\lambda_i x + \mu_i |_{x=c_i} = \frac{1}{c_i - r/K} \left(1 - \frac{r}{K}\right)^2 \quad (130)$$

$$= \frac{1}{i} \left(1 - \frac{r}{K}\right). \quad (131)$$

Notice that by (127), (129), and (131), the following three relationships hold:

$$\lambda_i = -\frac{1}{i(i-1)} < 0, \quad (132)$$

$$\mu_i = \frac{2}{i} \left(1 - \frac{r}{K}\right) + \frac{1}{i(i-1)} > 0, \quad (133)$$

$$\lambda_i + \mu_i = \frac{2}{i} \left(1 - \frac{r}{K}\right) > 0. \quad (134)$$

Moreover, by its convexity over $x \in [1, +\infty)$, the function $\frac{1}{x-r/K} \left(1 - \frac{r}{K}\right)^2 - (\lambda_i x + \mu_i)$ must be non-negative

outside of the interval formed by the two zeros, i.e.,

$$\frac{1}{x - r/K} \left(1 - \frac{r}{K}\right)^2 \geq \lambda_i x + \mu_i, \quad \forall x \in [1, c_{i-1}] \cup [c_i, \infty). \quad (135)$$

Therefore,

$$\frac{1}{c_j - r/K} \left(1 - \frac{r}{K}\right)^2 \geq \lambda_i c_j + \mu_i, \quad \forall j \in [K-1]. \quad (136)$$

Back to the converse, from (117), the communication load L is lower bounded as

$$L \geq \frac{H(X_K)}{NKT} \quad (137)$$

$$\stackrel{(a)}{\geq} \sum_{j=1}^{K-1} \frac{b_j}{NK} \cdot \frac{1}{j} \quad (138)$$

$$\stackrel{(b)}{=} \frac{1}{N(K-r)} \cdot \sum_{j=1}^{K-1} b_j \cdot \frac{1}{c_j - r/K} \left(1 - \frac{r}{K}\right)^2 \quad (139)$$

$$\stackrel{(c)}{\geq} \frac{1}{N(K-r)} \sum_{j=1}^{K-1} b_j (\lambda_i c_j + \mu_i) \quad (140)$$

$$= \frac{1}{N(K-r)} \sum_{j=1}^{K-1} b_j \left(\lambda_i \left(\left(1 - \frac{r}{K}\right) j + \frac{r}{K} \right) + \mu_i \right) \quad (141)$$

$$= \frac{1}{N(K-r)} \cdot \left(\lambda_i \left(1 - \frac{r}{K}\right) \cdot \sum_{j=1}^{K-1} j b_j + \left(\lambda_i \frac{r}{K} + \mu_i \right) \cdot \sum_{j=1}^{K-1} b_j \right) \quad (142)$$

$$= \frac{\lambda_i}{NK} \cdot \sum_{j=1}^{K-1} (j-1) b_j + \frac{\lambda_i + \mu_i}{N(K-r)} \cdot \sum_{j=1}^{K-1} b_j \quad (143)$$

$$\stackrel{(d)}{\geq} \frac{\lambda_i}{NK} \cdot (c-1)NK + \frac{\lambda_i + \mu_i}{N(K-r)} \cdot N(K-r) \quad (144)$$

$$= \lambda_i c + \mu_i \quad (145)$$

$$\stackrel{(e)}{=} -\frac{1}{i(i-1)}c - \frac{2}{Ki}r + \frac{2i-1}{i(i-1)}, \quad (146)$$

where (a) follows from Lemma 1 by setting $\mathcal{S} = \mathcal{K}$; (b) follows from (127); (c) follows from (136); (d) follows from (125), (126) and (132), (134); and (e) follows from (132), (133). Since the SCC triples P_{i-1} , P_i , and P_K defined in (32) satisfy inequality (146) with equality, the above inequalities indicate that all feasible triples (r, c, L) must lie above the plane containing $\triangle P_{i-1}P_iP_K$. Furthermore, the converse in [3] indicates that, for any c , we have (see Remark 2)

$$L \geq -\frac{1}{i(i+1)}r + \frac{1}{i} + \frac{1}{i+1} - \frac{1}{K}, \quad i \in [K-1], \quad (147)$$

which implies that all feasible triples (r, c, L) must lie above the plane containing P_1, P_2, Q_2 and the planes containing $P_i, P_{i+1}, Q_{i+1}, Q_i$, for $i = 2, \dots, K-1$, respectively. Hence, we conclude that (r, c, L) must lie on or above the surface \mathcal{F} .

B. Proof of Lemma 1

For notational brevity, we denote the tuple $(\mathcal{V}_S, \mathcal{C}_S)$ by Y_S for any $S \subseteq \mathcal{K}$. We prove Lemma 1 by mathematical induction on the size of S :

When $|S| = 1$, W.L.O.G, assume $S = \{k\}$, then (124) becomes

$$H(X_k | \mathcal{V}_{\mathcal{K} \setminus \{k\}}, \mathcal{C}_{\mathcal{K} \setminus \{k\}}) \geq 0, \quad (148)$$

which is trivial.

Suppose that, the statement is true for all subsets of \mathcal{K} with size s , $1 \leq s < K$. Consider a set $S \subseteq \mathcal{K}$ such that $|S| = s + 1$, then

$$H(X_S | Y_{S^c}) \quad (149)$$

$$= \frac{1}{|S|} \sum_{k \in S} H(X_S, X_k | Y_{S^c}) \quad (150)$$

$$= \frac{1}{|S|} \sum_{k \in S} (H(X_k | Y_{S^c}) + H(X_S | X_k, Y_{S^c})) \quad (151)$$

$$= \frac{1}{|S|} \sum_{k \in S} H(X_k | Y_{S^c}) + \frac{1}{|S|} \sum_{k \in S} H(X_S | X_k, Y_{S^c}) \quad (152)$$

$$\geq \frac{1}{|S|} H(X_S | Y_{S^c}) + \frac{1}{|S|} \sum_{k \in S} H(X_S | X_k, Y_{S^c}). \quad (153)$$

Then from (153), we have

$$H(X_S | Y_{S^c}) \quad (154)$$

$$= \frac{1}{|S| - 1} \sum_{k \in S} H(X_S | X_k, Y_{S^c}) \quad (155)$$

$$\geq \frac{1}{s} \sum_{k \in S} H(X_S | X_k, \mathcal{C}_k, Y_{S^c}) \quad (156)$$

$$\stackrel{(a)}{=} \frac{1}{s} \sum_{k \in S} H(X_S | \mathcal{C}_k, Y_{S^c}) \quad (157)$$

$$\stackrel{(b)}{=} \frac{1}{s} \sum_{k \in S} (H(X_S | \mathcal{C}_k, Y_{S^c}) + H(\mathcal{V}_k | X_S, \mathcal{C}_k, Y_{S^c})) \quad (158)$$

$$\stackrel{(c)}{=} \frac{1}{s} \sum_{k \in S} H(X_S, \mathcal{V}_k | \mathcal{C}_k, Y_{S^c}) \quad (159)$$

$$\stackrel{(d)}{=} \frac{1}{s} \sum_{k \in S} (H(\mathcal{V}_k | \mathcal{C}_k, Y_{S^c}) + H(X_S | \mathcal{V}_k, \mathcal{C}_k, Y_{S^c})), \quad (160)$$

where (a) follows from the fact that X_k is a function of \mathcal{C}_k ; (b) holds because

$$H(\mathcal{V}_k | X_S, \mathcal{C}_k, Y_{S^c}) = 0, \quad (161)$$

since \mathcal{V}_k can be decoded by \mathcal{C}_k, X_S and X_{S^c} , which is a function of Y_{S^c} ; and (c), (d) follows from chain rule.

We proceed to derive a lower bound for each term in (160). Firstly,

$$H(\mathcal{V}_k|\mathcal{C}_k, Y_{\mathcal{S}^c}) = H(\mathcal{V}_k|\mathcal{C}_k, \mathcal{V}_{\mathcal{S}^c}, \mathcal{C}_{\mathcal{S}^c}) \quad (162)$$

$$\stackrel{(a)}{=} H(\mathcal{V}_k|\mathcal{C}_k, \mathcal{C}_{\mathcal{S}^c}) \quad (163)$$

$$= H(\mathcal{V}_k|\mathcal{C}_{(\mathcal{S}\setminus\{k\})^c}) \quad (164)$$

$$\stackrel{(b)}{=} T \cdot \sum_{j=1}^{|\mathcal{S}|-1} b_{\mathcal{S},j}^k \quad (165)$$

$$= T \cdot \sum_{j=1}^s b_{\mathcal{S},j}^k, \quad (166)$$

where (a) follows from the independence between \mathcal{V}_k and $\mathcal{V}_{\mathcal{S}^c}$; and (b) holds because

$$\mathcal{B}_{\mathcal{S},1}^k, \dots, \mathcal{B}_{\mathcal{S},|\mathcal{S}|-1}^k \quad (167)$$

form a partition of those IVAs of \mathcal{V}_k that are not computed by any node in $(\mathcal{S}\setminus\{k\})^c$. Secondly,

$$H(X_{\mathcal{S}}|\mathcal{V}_k, \mathcal{C}_k, Y_{\mathcal{S}^c}) \quad (168)$$

$$= H(X_{\mathcal{S}\setminus\{k\}}, X_k|\mathcal{V}_k, \mathcal{C}_k, Y_{\mathcal{S}^c}) \quad (169)$$

$$\stackrel{(a)}{=} H(X_{\mathcal{S}\setminus\{k\}}|\mathcal{V}_k, \mathcal{C}_k, Y_{\mathcal{S}^c}) \quad (170)$$

$$= H(X_{\mathcal{S}\setminus\{k\}}|Y_{(\mathcal{S}\setminus\{k\})^c}) \quad (171)$$

$$\stackrel{(b)}{\geq} T \cdot \sum_{j=1}^{s-1} b_{\mathcal{S}\setminus\{k\},j} \cdot \frac{1}{j}, \quad (172)$$

where (a) follows from the fact that X_k is a function of \mathcal{C}_k ; and (b) follows from the induction assumption.

Finally, combining (160), (166) and (172), we have

$$H(X_{\mathcal{S}}|Y_{\mathcal{S}^c}) \quad (173)$$

$$\geq \frac{1}{s} \sum_{k \in \mathcal{S}} H(\mathcal{V}_k|\mathcal{C}_k, Y_{\mathcal{S}^c}) + \frac{1}{s} \sum_{k \in \mathcal{S}} H(X_{\mathcal{S}}|\mathcal{V}_k, \mathcal{C}_k, Y_{\mathcal{S}^c}) \quad (174)$$

$$\geq \frac{T}{s} \sum_{k \in \mathcal{S}} \sum_{j=1}^s b_{\mathcal{S},j}^k + \frac{T}{s} \sum_{k \in \mathcal{S}} \sum_{j=1}^{s-1} b_{\mathcal{S}\setminus\{k\},j} \cdot \frac{1}{j} \quad (175)$$

$$= \frac{T}{s} \sum_{j=1}^s \sum_{k \in \mathcal{S}} b_{\mathcal{S},j}^k + \frac{T}{s} \sum_{j=1}^{s-1} \sum_{k \in \mathcal{S}} b_{\mathcal{S}\setminus\{k\},j} \cdot \frac{1}{j} \quad (176)$$

$$\stackrel{(a)}{=} \frac{T}{s} \sum_{j=1}^s b_{\mathcal{S},j} + \frac{T}{s} \sum_{j=1}^{s-1} \sum_{k \in \mathcal{S}} b_{\mathcal{S}\setminus\{k\},j} \cdot \frac{1}{j}, \quad (177)$$

where (a) follows from (123).

Let $\mathbb{I}(A)$ be the indicator function of an event A , i.e.,

$$\mathbb{I}(A) = \begin{cases} 1, & \text{if } A \text{ is true} \\ 0, & \text{if } A \text{ is false} \end{cases}, \quad (178)$$

Then,

$$\sum_{k \in \mathcal{S}} b_{\mathcal{S} \setminus \{k\}, j} \quad (179)$$

$$\stackrel{(a)}{=} \sum_{k \in \mathcal{S}} \sum_{l \in \mathcal{S} \setminus \{k\}} b_{\mathcal{S} \setminus \{k\}, j}^l \quad (180)$$

$$= \sum_{l \in \mathcal{S}} \sum_{k \in \mathcal{S} \setminus \{l\}} b_{\mathcal{S} \setminus \{k\}, j}^l \quad (181)$$

$$\stackrel{(b)}{=} \sum_{l \in \mathcal{S}} \sum_{k \in \mathcal{S} \setminus \{l\}} \sum_{n=1}^N \mathbb{I}(v_{l,n} \text{ is only computed by } j \text{ nodes in } \mathcal{S} \setminus \{k, l\}) \quad (182)$$

$$= \sum_{l \in \mathcal{S}} \sum_{k \in \mathcal{S} \setminus \{l\}} \sum_{n=1}^N \mathbb{I}(v_{l,n} \text{ is only computed by } j \text{ nodes in } \mathcal{S} \setminus \{l\}) \cdot \mathbb{I}(v_{l,n} \text{ is not computed by node } k) \quad (183)$$

$$= \sum_{l \in \mathcal{S}} \sum_{n=1}^N \mathbb{I}(v_{l,n} \text{ is only computed by } j \text{ nodes in } \mathcal{S} \setminus \{l\}) \cdot \sum_{k \in \mathcal{S} \setminus \{l\}} \mathbb{I}(v_{l,n} \text{ is not computed by node } k) \quad (184)$$

$$= \sum_{l \in \mathcal{S}} \sum_{n=1}^N \mathbb{I}(v_{l,n} \text{ is only computed by } j \text{ nodes in } \mathcal{S} \setminus \{l\}) \cdot (s - j) \quad (185)$$

$$\stackrel{(c)}{=} \sum_{l \in \mathcal{S}} b_{\mathcal{S}, j}^l (s - j) \quad (186)$$

$$\stackrel{(d)}{=} b_{\mathcal{S}, j} (s - j), \quad (187)$$

where (a), (d) follows from (123), and (b), (c) follows from the definition of $b_{\mathcal{S} \setminus \{k\}, j}^l$ and $b_{\mathcal{S}, j}^l$ respectively.

Therefore, from (177) and (187),

$$H(X_{\mathcal{S}} | Y_{\mathcal{S}^c}) \quad (188)$$

$$\geq \frac{T}{s} \cdot \sum_{j=1}^s b_{\mathcal{S}, j} + \frac{T}{s} \cdot \sum_{j=1}^{s-1} \sum_{k \in \mathcal{S}} b_{\mathcal{S} \setminus \{k\}, j} \cdot \frac{1}{j} \quad (189)$$

$$= \frac{T}{s} \cdot \sum_{j=1}^s b_{\mathcal{S}, j} + \frac{T}{s} \cdot \sum_{j=1}^{s-1} b_{\mathcal{S}, j} \cdot \frac{s-j}{j} \quad (190)$$

$$= \frac{T}{s} \cdot \sum_{j=1}^s b_{\mathcal{S}, j} + T \cdot \sum_{j=1}^{s-1} \frac{b_{\mathcal{S}, j}}{j} - \frac{T}{s} \cdot \sum_{j=1}^{s-1} b_{\mathcal{S}, j} \quad (191)$$

$$= T \cdot \frac{b_{\mathcal{S}, s}}{s} + T \cdot \sum_{j=1}^{s-1} \frac{b_{\mathcal{S}, j}}{j} \quad (192)$$

$$= T \cdot \sum_{j=1}^{|\mathcal{S}|-1} \frac{b_{\mathcal{S}, j}}{j}. \quad (193)$$

Notice that, we have proved that (124) holds for all $\mathcal{S} \subseteq \mathcal{K}$ with $|\mathcal{S}| = s + 1$. By the principle of mathematical induction, we conclude that (124) holds for all nonempty subsets $\mathcal{S} \subseteq \mathcal{K}$.

C. Proof of Lemma 2

For any $k \in \mathcal{K}$, define

$$\tilde{\mathcal{B}}_k \triangleq \{v_{k,n} : v_{k,n} \text{ is computed by node } k\}, \quad (194)$$

i.e., $\tilde{\mathcal{B}}_k$ is the set of IVAs for the output function ϕ_k that are computed by node k . Denote the cardinality of $\tilde{\mathcal{B}}_k$ by \tilde{b}_k . Notice that,

$$\tilde{\mathcal{B}}_k, \mathcal{B}_{\mathcal{K},1}^k, \mathcal{B}_{\mathcal{K},2}^k, \dots, \mathcal{B}_{\mathcal{K},K-1}^k \quad (195)$$

forms a partition of IVAs \mathcal{V}_k . Thus,

$$\tilde{b}_k + \sum_{j=1}^{K-1} b_{\mathcal{K},j}^k = |\mathcal{V}_k| = N. \quad (196)$$

Therefore, summing over $k \in \mathcal{K}$ in (196), together with (123),

$$\sum_{k=1}^K \tilde{b}_k + \sum_{j=1}^{K-1} b_j = NK. \quad (197)$$

Moreover, since each node k must store file w_n when $v_{k,n} \in \tilde{\mathcal{B}}_k$, we have $\tilde{b}_k \leq |\mathcal{M}_k|$, and by (115),

$$\sum_{k=1}^K \tilde{b}_k \leq \sum_{k=1}^K |\mathcal{M}_k| = rN. \quad (198)$$

Also, for $k \in \mathcal{K}$ and $j \in [K-1]$, IVAs $\tilde{\mathcal{B}}_k$ must be computed at node k , and IVAs $\mathcal{B}_{\mathcal{K},j}^k$ must be computed at j nodes. Thus by (116),

$$\sum_{k=1}^K \tilde{b}_k + \sum_{j=1}^{K-1} j b_j \leq \sum_{k=1}^K |\mathcal{C}_k| = cNK. \quad (199)$$

Combining (197) with (198) and (199) respectively, yield (125) and (126).

APPENDIX C

PROOF OF OPTIMAL TRADEOFF SURFACE IN THEOREM 1

We now prove that \mathcal{O} is the optimal tradeoff surface of the region \mathcal{R} . Obviously, all pareto-optimal points must lie on the surface \mathcal{F} . Since the triangle $\triangle P_1 P_2 Q_2$ and the trapezoids $\square P_i Q_i Q_{i+1} P_{i+1}$ ($i \in [2 : K-1]$) are parallel to \vec{e}_2 , all points in the interior of these facets cannot be pareto-optimal. In the following, we prove that, all the points on the triangles $\triangle P_{i-1} P_i P_K$ ($i \in [2 : K-1]$) must be pareto-optimal.

For any (r, c) satisfying (23a), let $L^*(r, c)$ be the function such that $(r, c, L^*(r, c)) \in \mathcal{F}$. Then by (146), it has strictly positive directional derivative in any direction $(r \leq 0, c \leq 0)$ in the interior of the projection of $\triangle P_{i-1} P_i P_K$ on the (r, c) plane.

Fix now a triple $(r, c, L^*(r, c)) \in \mathcal{O}$. We show that it is pareto-optimal. To this end, consider any other triple $(r', c', L') \in \mathcal{R}$ that satisfies

$$r' \leq r, \quad c' \leq c, \quad L' \leq L^*(r, c). \quad (200)$$

We show by contradiction that all three inequalities must hold with equality. We distinguish between triples (r', c', L') for which

$$(r', c', L^*(r', c')) \in \mathcal{O}, \quad (201)$$

and triples where this is not the case.

- 1) Assume that (201) holds. If $r' = r$ and $c' = c$, then obviously, $L' \geq L^*(r, c)$, thus all equalities in (200) hold. If $r' < r$ or $c' < c$, then

$$L^*(r', c') > L^*(r, c), \quad (202)$$

simply because the directional derivative along $(r' - r, c' - c)$ is strictly positive by (146). Since $(r', c', L') \in \mathcal{R}$, we have $L' \geq L^*(r', c')$ and thus by (202), $L' > L^*(r, c)$, which contradicts (200).

- 2) Assume now that (201) is violated. Then, $(r', c', L^*(r', c'))$ must lie on at least one of the $K - 1$ facets

$$\triangle P_1 P_2 Q_2 \quad \text{or} \quad \triangle P_i Q_i Q_{i+1} P_{i+1}, \quad i = 2, \dots, K - 1. \quad (203)$$

As they are all parallel to \vec{e}_2^λ , there exists $c'' < c' \leq c$ such that, $(r', c'', L^*(r', c'')) \in \mathcal{O}$ and $L^*(r', c'') = L^*(r', c')$. Therefore,

$$L' \geq L^*(r', c') = L^*(r', c'') \stackrel{(a)}{>} L^*(r, c), \quad (204)$$

where (a) follows by proof step 1). But (204) contradicts with (200).

From the above analysis, we conclude that, any point on \mathcal{O} is pareto-optimal.

APPENDIX D

PROOF OF THEOREM 3

Recall that an achievable SCC triple (r, c, L) is on $\triangle P_{g-1} P_g P_K$ if, and only if, (r, c, L) satisfies

$$L = -\frac{1}{g(g-1)}c - \frac{2}{Kg}r + \frac{2g-1}{g(g-1)}. \quad (205)$$

Thus, we need to show that (r_A, c_A, L_A) is on the plane in (205) if, and only if, $\theta_t = 0, \forall t \in [2 : K] \setminus \{g, g+1\}$.

Let S_t be the number of ordinary symbols having occurrence t , and θ_t be the fraction of the entries having occurrence t among all non-“*” entries. For each $t \in [2 : K]$, define

$$\left(c_A^{(t)}, L_A^{(t)}\right) = \left(\frac{Z}{F} + \left(1 - \frac{Z}{F}\right)(t-1), \frac{1}{t-1} \left(1 - \frac{Z}{F}\right)\right). \quad (206)$$

Notice that, all the points $(c_{\mathbf{A}}^{(t)}, L_{\mathbf{A}}^{(t)})$ for $t \in [2 : K]$ lie on the curve

$$c \mapsto L(c) = \frac{1}{c - Z/F} \left(1 - \frac{Z}{F}\right)^2, \quad (207)$$

which is convex for $c > \frac{Z}{F}$. Define

$$\beta_g \triangleq -\frac{1}{g(g-1)}, \quad (208a)$$

$$\gamma_g \triangleq \frac{2}{g} \left(1 - \frac{Z}{F}\right) + \frac{1}{g(g-1)}. \quad (208b)$$

and notice further that

$$\beta_g c_{\mathbf{A}}^{(g)} + \gamma_g = L_{\mathbf{A}}^{(g)} \quad (209)$$

$$\beta_g c_{\mathbf{A}}^{(g+1)} + \gamma_g = L_{\mathbf{A}}^{(g+1)}. \quad (210)$$

That means, the line $y = \beta_g x + \gamma_g$ passes through the points $(c_{\mathbf{A}}^{(g)}, L_{\mathbf{A}}^{(g)})$ and $(c_{\mathbf{A}}^{(g+1)}, L_{\mathbf{A}}^{(g+1)})$. By the convexity of the function in (207), this implies that

$$\frac{1}{c - Z/F} \left(1 - \frac{Z}{F}\right)^2 \geq \beta_g c + \gamma_g, \quad \forall c \in [1, c_{\mathbf{A}}^{(g)}] \cup [c_{\mathbf{A}}^{(g+1)}, \infty), \quad (211)$$

with equality if, and only if, $x = c_{\mathbf{A}}^{(g)}$ or $x = c_{\mathbf{A}}^{(g+1)}$. Therefore,

$$\frac{1}{c_{\mathbf{A}}^{(t)} - Z/F} \left(1 - \frac{Z}{F}\right)^2 \geq \beta_g c_{\mathbf{A}}^{(t)} + \gamma_g, \quad \forall t \in [2 : K], \quad (212)$$

with equality if, and only if, $t = g$ or $t = g + 1$.

By Theorem 2, we have

$$r_{\mathbf{A}} = \frac{KZ}{F}, \quad (213a)$$

$$c_{\mathbf{A}} = \sum_{t=2}^K \theta_t c_{\mathbf{A}}^{(t)}, \quad (213b)$$

$$L_{\mathbf{A}} = \sum_{t=2}^K \theta_t L_{\mathbf{A}}^{(t)}, \quad (213c)$$

which implies

$$L_{\mathbf{A}} \stackrel{(a)}{=} \sum_{t=2}^K \theta_t L_{\mathbf{A}}^{(t)} \quad (214)$$

$$\stackrel{(b)}{=} \sum_{t=2}^K \theta_t \cdot \frac{1}{c_{\mathbf{A}}^{(t)} - Z/F} \left(1 - \frac{Z}{F}\right)^2 \quad (215)$$

$$\stackrel{(c)}{\geq} \sum_{t=2}^K \theta_t \cdot (\beta_g c_{\mathbf{A}}^{(t)} + \gamma_g) \quad (216)$$

$$= \beta_g \sum_{t=2}^K \theta_t c_{\mathbf{A}}^{(t)} + \gamma_g \quad (217)$$

$$\stackrel{(d)}{=} \beta_g c_{\mathbf{A}} + \gamma_g \quad (218)$$

$$\stackrel{(e)}{=} -\frac{1}{g(g-1)}c_{\mathbf{A}} + \frac{2}{g}\left(1 - \frac{Z}{F}\right) + \frac{1}{g(g-1)} \quad (219)$$

$$\stackrel{(f)}{=} -\frac{1}{g(g-1)}c_{\mathbf{A}} - \frac{2}{Kg}r_{\mathbf{A}} + \frac{2g-1}{g(g-1)}, \quad (220)$$

where (a), (d), (f) follow from (213); (b) follows from the fact that $(c_{\mathbf{A}}^{(t)}, L_{\mathbf{A}}^{(t)})$ lies on the curve in (207); (c) follows from (212); and (e) follows from (208).

Notice that, (220) implies that $(r_{\mathbf{A}}, c_{\mathbf{A}}, L_{\mathbf{A}})$ lies on the plane (205) if, and only if, (216) holds with equality, which is equivalent to $\theta_t = 0, \forall t \in [2 : K] \setminus \{g, g+1\}$ by (212). This concludes the proof of the first part.

We proceed to prove (98) when all ordinary symbols in \mathbf{A} have occurrence either g or $g+1$. Let S_g be the number of ordinary symbols that occur g times. Counting the number of non-“*” entries in \mathbf{A} , we have

$$S_g g + (S - S_g)(g+1) = K(F - Z). \quad (221)$$

The fraction of non-“*” entries of \mathbf{A} having occurrence g is thus

$$\theta = \frac{S_g g}{K(F - Z)} \quad (222)$$

$$= \frac{S_g(g+1)}{K(F - Z)} - g, \quad (223)$$

and the fraction of non-“*” entries of \mathbf{A} having occurrence $g+1$ is $1 - \theta$. Plugging these expressions into Theorem 2 proves achievability of the SCC triple

$$(r_{\mathbf{A}}, c_{\mathbf{A}}, L_{\mathbf{A}}) = \left(\frac{KZ}{F}, \frac{Z}{F} + \left(1 - \frac{Z}{F}\right)(\theta(g-1) + (1-\theta)g), \left(\frac{\theta}{g-1} + \frac{1-\theta}{g}\right)\left(1 - \frac{Z}{F}\right) \right) \quad (224)$$

$$= \left(\frac{KZ}{F}, \frac{Z}{F} + \left(1 - \frac{Z}{F}\right)(g - \theta), \frac{g-1+\theta}{g(g-1)}\left(1 - \frac{Z}{F}\right) \right). \quad (225)$$

This concludes the proof.

REFERENCES

- [1] J. Dean and S. Ghemawat, “MapReduce: Simplified data processing on large clusters,” *Sixth USENIX OSDI*, Dec. 2004.
- [2] M. Isard, M. Budiu, Y. Yu, A. Birrell, and D. Fetterly, “Dryad: distributed data-parallel programs from sequential building blocks,” in *Proc. the 2nd ACM SIGOPS/EuroSys’07*, Mar. 2007.
- [3] S. Li, M. A. Maddah-Ali, Q. Yu, and A. S. Avestimehr, “A fundamental tradeoff between computation and communication in distributed computing,” *IEEE Trans. Inf. Theory*, vol. 64, no. 1, pp. 109–128, Jan. 2018.
- [4] Y. H. Ezzeldin, M. Karmoose, and C. Fragouli, “Communication vs distributed computation: An alternative trade-off curve,” in *Proc. IEEE Inf. Theory Workshop (ITW)*, Kaohsiung, Taiwan, pp. 279–283, Nov. 2017.
- [5] K. Lee, M. Lam, R. Pedarsani, D. Papailiopoulos, and K. Ramchandran, “Speeding up distributed machine learning using codes,” *IEEE Trans. Inf. Theory*, vol. 64, no. 3, pp. 1514–1529, Mar. 2018.
- [6] S. Li, M. A. Maddah-Ali, and A. S. Avestimehr, “A unified coding framework for distributed computing with straggling servers,” in *Proc. IEEE Globecom Works (GC Wkshps)*, Washington, DC, USA, Dec. 2016.
- [7] A. Reisizadeh, S. Prakash, R. Pedarsani, and S. Avestimehr, “Coded computation over heterogeneous clusters,” in *Proc. IEEE Int. Symp. Inf. Theory*, Aachen, Germany, pp. 2408–2412, Jun. 2017.
- [8] Q. Yu, M. Maddah-Ali, and S. Avestimehr, “Polynomial codes: An optimal design for high-dimensional coded matrix multiplication,” in *Proc. The 31st Annual Conf. Neural Inf. Processing System (NIPS)*, Long Beach, CA, USA, May 2017.

- [9] Q. Yu, M. Maddah-Ali, and S. Avestimehr, "Straggler mitigation in distributed matrix multiplication: Fundamental limits and optimal coding," in *Proc. IEEE Int. Symp. Inf. Theory*, Vail, CO, USA, pp. 2022–2026, Jun. 2018.
- [10] K. Lee, C. Suh, and K. Ramchandran, "High-dimensional coded matrix multiplication," in *Proc. IEEE Int. Symp. Inf. Theory*, Aachen, Germany, pp. 2418–2422, Jun. 2017.
- [11] H. Park, K. Lee, J. Sohn, C. Suh, and J. Moon, "Hierarchical coding for distributed computing," arXiv:1801.04686.
- [12] F. Haddadpour and V. R. Cadambe, "Codes for distributed finite alphabet matrix-vector multiplication," in *Proc. IEEE Int. Symp. Inf. Theory*, Vail, CO, USA, pp. 1625–1629, Jun. 2018.
- [13] S. Kiani, N. Ferdinand and S. C. Draper, "Exploitation of stragglers in coded computation," in *Proc. IEEE Int. Symp. Inf. Theory*, Vail, CO, USA, pp. 1988–1992, Jun. 2018.
- [14] T. Baharav, K. Lee, O. Ocal, and K. Ramchandran, "Straggler-proofing massive-scale distributed matrix multiplication with d -dimensional product codes," in *Proc. IEEE Int. Symp. Inf. Theory*, Vail, CO, USA, pp. 1993–1997, Jun. 2018.
- [15] N. Ferdinand and S. C. Draper, "Hierarchical coded computation," in *Proc. IEEE Int. Symp. Inf. Theory*, Vail, CO, USA, pp. 1620–1624, Jun. 2018.
- [16] Q. Yu, S. Li, M. A. Maddah-Ali, and A. S. Avestimehr, "How to optimally allocate resources for coded distributed computing," in *Proc. IEEE Int. Conf. Commun. (ICC)*, 2017, Paris, France, 21–25, May 2017.
- [17] S. Li, Q. Yu, M. A. Maddah-Ali, and A. S. Avestimehr, "A scalable framework for wireless distributed computing," *IEEE/ACM Trans. Netw.*, vol. 25, no. 5, pp. 2643–2653, Oct. 2017.
- [18] S. Li, Q. Yu, M. A. Maddah-Ali, and A. S. Avestimehr, "Edge-facilitated wireless distributed computing," in *Proc. IEEE Glob. Commun. Conf. (Globcom)*, Washington, DC, USA, Dec. 2016.
- [19] F. Li, J. Chen, and Z. Wang, "Wireless Mmap-Reduce distributed computing," in *Proc. IEEE Int. Symp. Inf. Theory*, Vail, CO, USA, pp. 1286–1290, Jun. 2018.
- [20] E. Parrinello, E. Lampir, and P. Elia, "Coded distributed computing with node cooperation substantially increases speedup factors," in *Proc. IEEE Int. Symp. Inf. Theory*, Vail, CO, USA, pp. 1291–1295, Jun. 2018.
- [21] M. A. Attia and R. Tandon, "On the worst-case communication overhead for distributed data shuffling," in *Proc. 54th Allerton Conf. Commun., Control, Comput.*, Monticello, IL, USA, pp. 961–968, Sep. 2016.
- [22] M. A. Attia and R. Tandon, "Information theoretic limits of data shuffling for distributed learning," in *Proc. IEEE Glob. Commun. Conf. (Globcom)*, Washington, DC, USA, Dec. 2016.
- [23] A. Elmahdy and S. Mohajer, "On the fundamental limits of coded data shuffling," in *Proc. IEEE Int. Symp. Inf. Theory*, Vail, CO, USA, pp. 716–720, Jun. 2018.
- [24] L. Song, S. R. Srinivasavaradhan, and C. Fragouli, "The benefit of being flexible in distributed computation," in *Proc. IEEE Inf. Theory Workshop (ITW)*, Kaohsiung, Taiwan, pp. 289–293, Nov. 2017.
- [25] S. R. Srinivasavaradhan, L. Song, and C. Fragouli, "Distributed computing trade-offs with random connectivity," in *Proc. IEEE Int. Symp. Inf. Theory*, Vail, CO, USA, pp. 1281–1285, Jun. 2018.
- [26] R. Tandon, Q. Lei, A. G. Dimakis, and N. Karampatziakis, "Gradient coding: Avoiding stragglers in synchronous gradient descent," arXiv: 1612.03301.
- [27] N. Raviv, I. Tamo, R. Tandon, and A. G. Dimakis, "Gradient coding from cyclic MDS codes and expander graphs," arXiv: 1707.03858.
- [28] Z. Charles and D. Papailiopoulos, "Gradient coding using the stochastic block model," in *Proc. IEEE Int. Symp. Inf. Theory*, Vail, CO, USA, pp. 1998–2002, Jun. 2018.
- [29] W. Halbawi, N. Azizan, F. Salehi, and B. Hassil, "Improving distributed gradient descent using Reed-Solomon codes," in *Proc. IEEE Int. Symp. Inf. Theory*, Vail, CO, USA, pp. 2027–2031, Jun. 2018.
- [30] M. A. Maddah-Ali and U. Niesen, "Fundamental limits of caching," *IEEE Trans. Inf. Theory*, vol. 60, no. 5, pp. 2856–2867, May 2014.
- [31] Q. Yan, M. Cheng, X. Tang, and Q. Chen, "On the placement delivery array design for centralized coded caching scheme," *IEEE Trans. Inf. Theory*, vol. 63, no. 9, pp. 5821–5833, Sep. 2017.
- [32] C. Shangguan, Y. Zhang, and G. Ge, "Centralized coded caching schemes: A hypergraph theoretical approach," *IEEE Trans. Inf. Theory*, vol. 64, no. 8, pp. 5755–5766, Aug. 2018.
- [33] Q. Yan, S. Yang, and M. Wigger, "A storage-computation-communication tradeoff for distributed computing," in *Proc. Int. Symp. Wireless Commun. Systems*, Lisbon, Portugal, Aug. 2018.
- [34] Q. Yan, X. Tang, Q. Chen, and M. Cheng, "Placement delivery array design through strong edge coloring of bipartite graphs," *IEEE Commun. Lett.*, vol. 22, no. 2, pp. 236–239, Feb. 2018.